Research Square

Preprints are preliminary reports that have not undergone peer review.
They should not be considered conclusive, used to inform clinical practice,
or referenced by the media as validated information.

Bi-directional Coupling of an Unstructured Triangular Meshes-based Integrated Hydrodynamic Model for Heterogeneous Feature-based Urban Flood Simulation

Guoqiang Peng (Geop1987@gmail.com)
Shaanxi Normal University https://orcid.org/0000-0002-7351-6222
Zhuo Zhang
Nanjing Normal University
Tian Zhang
Shaanxi Normal University
Zhiyao Song
Nanjing Normal University
Arif Masrur
The Pennsylvania State University

Research Article

Keywords: Spatial heterogeneity, Geographic modelling, Comprehensive analysis

Posted Date: April 1st, 2021

DOI: https://doi.org/10.21203/rs.3.rs-375226/v1

License: This work is licensed under a Creative Commons Attribution 4.0 International License.
Read Full License

Version of Record: A version of this preprint was published at Natural Hazards on August 22nd, 2021. See the published version at https://doi.org/10.1007/s11069-021-04966-5.

Bi-directional coupling of an unstructured triangular meshes-based integrated hydrodynamic model for heterogeneous feature-based urban flood simulation

Guoqiang Peng [1,2,3,4]*, Zhuo Zhang [2,3], Tian Zhang[1], Zhiyao Song [2,3] and Arif Masrur [4]

[1] School of Geography and Tourism, Shaanxi Normal University, Xi'an 710062, Shaanxi, China
[2] Key Laboratory of Virtual Geographic Environment (Ministry of Education), Nanjing Normal University, Nanjing 210023, China
[3] Jiangsu Center for Collaborative Innovation in Geographical Information Resource Development and Application, Nanjing 210023, China
[4] GeoVISTA Center, College of Earth and Mineral Sciences, The Pennsylvania State University, State College, PA 16802, USA
Corresponding Author Email: geop1987@gmail.com

Abstract: Urban pluvial flash floods have become a matter of widespread concern, as they severely impact people's lives in urban areas. Hydrological and hydraulic models have been widely used for urban flood management and urban planning. Traditionally, to reduce the complexity of urban flood modelling and simulations, simplification or generalization methods have been used; for example, some models focus on the simulation of overland water flow, and some models focus on the simulation of the water flow in sewer systems. However, the water flow of urban floods includes both overland flow and sewer system flow. The overland flow processes are impacted by many different geographical features in what is an extremely spatially heterogeneous environment. Therefore, this article is based on two widely used models (SWMM and ANUGA) that are coupled to develop a bi-directional method of simulating water flow processes in urban areas. The open source overland flow model uses the unstructured triangular as the spatial discretization scheme. The unstructured triangular-based hydraulic model can be better used to capture the spatial heterogeneity of the urban surfaces. So, the unstructured triangular-based model is an essential condition for heterogeneous feature-based urban flood simulation. The experiments indicate that the proposed coupled model in this article can accurately depict surface waterlogged areas and that the heterogeneous feature-based urban flood model can be used to determine different types of urban flow processes.

Keywords: Spatial heterogeneity; Geographic modelling; Comprehensive analysis

1. Introduction

With the processes of urbanization and global climate change, urban floods are occurring more frequently, severely damaging property and endangering human lives. In China, many cities have

surveyed pluvial flash floods (PFFs) (Jiang et al., 2017, Sang et al., 2017). Hydrological models are widely used for urban water and disaster management and provide an efficient way to simulate the motion processes of floods and predict flood-caused consequences in urban areas (Mignot et al., 2006; Wang et al., 2018). Urban areas are extremely complex and heterogeneous, with many natural and man-made features, and the complex interactions in these areas affect the PFF process (Leandro et al., 2016; Xiao et al., 2017). Therefore, it is essential to construct an integrated model to support feature-based simulation and analysis.

The geographical features in an urban area typically include a list of diverse entities, such as buildings, roads, and lakes. The main types of hydrographic features in sewer systems include nodes (manholes, outfalls, etc.), pipelines, culverts, channels, weirs, and storage reservoirs. All the heterogeneous characteristics that influence urban floods in urban areas can be compiled and organized by features in geo-databases (Gong et al., 2017); for example, the features of a building might include the height, footprint coordinates, spatial relationships between manholes and the building, roof type, etc. Geographic features are the basic unit affecting hydrological processes in urban areas, and these features are the basic unit linked to human activities. From the aspect of GIS data management, features are the basic units of vector data layers (Zhang et al., 2016; Goodchild, M. F., 2018). Therefore, the widely used GIS data format can be used to conduct feature-based hydrodynamic modelling and simulations. The functions of a hydrological model must support flow calculations in different motion environments, such as overland flow in different land cover areas, sewer system flows, and the interactions between the surface and sewer water systems. The model initial conditions and border conditions are inputted from these basic geographical information data and parameters, such as terrain parameters and parameters of sewer nodes. Additionally, many other user-adjustable parameters control the model simulation effects, such as the Manning coefficient and loss coefficient.

To improve the integrated simulations of urban flood processes and consider the interactions between overland flow and sewer systems, many coupled and integrated models have been proposed. Some researchers have used dynamic link library technology to couple LISFLOOD and SWMM (Wu et al., 2017). However, LISFLOOD uses structured mesh grids for spatial discretization, and structured mesh schemes are not convenient for capturing the heterogeneous details of features. Additionally, many other coupled models have been proposed, such as those based on SIPSON and SWMM or on MESHSIM and SWMM. These models have been used to

support coupled simulations of overland flow and sewer systems. Many other researchers have used different numerical algorithms (e.g., the finite volume method, finite difference method, and Riemann discontinuities) to solve shallow water models and overland flow models. These researchers have developed proprietary models to more effectively perform interactive simulations of overland flow and sewer systems. Moreover, 1D/2D coupled urban flood models have been used to perform urban flooding simulations in recent years (Chang et al.,2015; Leandro et al., Lee et al., 2016; Chen et al., 2018; Martins et al., 2018). In these studies, buildings and roads were considered from input data, but buildings were not considered as interior holes, and the lakes were not treated as an independent feature. Yin et al. (2016) studied the impact and risk of PFFs on intra-urban road networks; this research used a parameterization solution to consider sewer systems. The existing coupled modelling studies and their considerations of spatial heterogeneity are shown in Table 1.

Table 1. The considerations of spatial heterogeneity in coupled models

Model	The considerations of spatial heterogeneity
LISFLOOD-SWMM	Digital elevation model (DEM)-based 2D hydraulic model coupled with SWMM (Wu et al.,2018); the DEM cannot be embedded with some geographical features, so the expressions of heterogeneity of the urban surface are based on land uses
SIPSON-SWMM	DEM-based 2D hydraulic model coupled with SWMM; the heterogeneity of the urban surface is based on land uses (Djordjević et al., 2005)
MESHSIM-SWMM	Uses a regular quadrangle approach to implement surface discretization; the surface heterogeneity, especially for features, is not effectively considered (Dey et al.,2007)
OFM-SWMM	Proprietary 2D hydraulic models developed and coupled with the OFM; however, they do not consider other features, such as the water flow in lakes, roads, and buildings (Chang et al.,2015; Lee et al., 2016)
SWM-SWMM	Proprietary 2D hydraulic model developed based on the SWM to consider the heterogeneity of the surface based on the land use type (Leandro et al., 2016; Chen et al., 2018); However, flow features are not independently considered
FloodMap-HydroInundation2D	High-resolution DEM-based 2D hydraulic model that considers the heterogeneity of roads (concave effect of road edges) but does not consider other surface features; uses a parameterization method to consider the sewer system (Yin et al., 2016)

However, no triangular mesh-based open-source 2D hydraulic model has been coupled with SWMM in the previous research. Unstructured triangular meshes can be used in spatial discretization schemes and support variations in the cell size to capture the details of spatial heterogeneity in certain areas. Additionally, adaptive-scale mesh grids can save computational

resources in some homogeneous areas. These advantages of unstructured triangular meshes are essential for heterogeneous feature-based hydraulic modelling and simulation. Therefore, this article proposes a spatial discretization method to consider the main heterogeneous features (e.g., roads, buildings, ponds, ditches, and land use types) and their characteristics in urban areas. An SWMM and ANUGA bi-directional coupled model simulation method is developed to simulate hydrological processes at the surface and in sewer systems.

The remainder of this article is organized as follows. Section 2 introduces the methodologies used to support the experiments. Section 3 illustrates the case study description. Section 4 introduces the experiment. The results and discussion are given in Section 5.

2. Methodology

2.1 Models

2.1.1. 2D hydraulic model

ANUGA Hydro is a 2D open-source hydraulic modelling system that supports the simulation of different scenarios and hydraulic processes, such as tsunamis, fluvial floods, dam breaks and rainstorm floods (Roberts et al., 2010). ANUGA was developed in a Python and C mixed programming language. Specifically, the core computation programs were developed in Python, and the input/output data programs were developed in C. The computation mechanisms of ANUGA are based on the finite volume method and Riemann discontinuities to solve the shallow water wave equation (SWWE). This equation can be expressed as follows (Zoppou et al., 1999):

$$\frac{\partial U}{\partial t} + \Delta \bullet \mathrm{F} = \mathrm{S} \quad (1)$$

where U represents the vector of conservative variables, F represents the flow tensor, and S represents the vector of source items. The Cartesian expression of the SWWE is as follows:

$$\frac{\partial U}{\partial t} + \frac{\partial E}{\partial x} + \frac{\partial G}{\partial y} = \mathrm{S} \quad (2)$$

where E and G are the Cartesian coordinate components of F.

ANUGA is one of very few open-source hydrodynamic model systems that can support 2D hydraulic simulations based on unstructured triangular meshes. The computations involving the 2D SWWE would be very complex if based on unstructured triangular mesh cells (Zoppou et al., 1999; Nielsen et al., 2005). ANUGA can calculate the water depth, flux and velocity for each cell

at each simulation step and perform integrated computations for discretized meshes to support flow analyses for different features (Mungkasi et al., 2013; 2015). The latest version of ANUGA was used to perform the overland flow simulations in this article.

2.1.2. 1D sewer model

SWMM, which was developed by the US EPA, was selected to simulate the sewer system (Gironás et al., 2010). SWMM is the most popular open-source model for urban storm water management and has been updated many times. This paper uses the official version of SWMM, which was developed in the C programming language. The main processes simulated in SWMM include the convergence of overland flow, water movement in sewer systems and sewage transportation. SWMM-EXTRAN, the sewer simulation module of SWMM, can effectively simulate the water flow in a sewer system (Hassan et al., 2017). The routing types for a sewer system include steady flow, kinematic wave, and dynamic wave models. Among these routing models, the dynamic wave routing model is the most powerful and can support simulations of very complex flow processes, such as import and export loss, pressure flows, multiple intersection flows, and circulation pipeline network flows. Therefore, the experiment in this article uses the dynamic wave routing model. The version of the model used in this article is SWMM-EXTRAN 5.1. SWMM-EXTRAN solves the full Saint-Venant equations to calculate the water movement in a sewer system (Rossman., 2010).

Mass conservation equation: $$\frac{\partial A}{\partial t} + \frac{\partial Q}{\partial x} = 0 \quad (3)$$

Momentum conservation equation: $$\frac{1}{g}\frac{\partial V}{\partial t} + \frac{V}{g}\frac{\partial V}{\partial x} + \frac{\partial H}{\partial x} = s_0 - s_f - h_L \quad (4)$$

where H represents the water surface height [m]; x is the pipeline length [m], A is the cross-sectional area [m^2]; V is the average flow velocity at the cross section [m/s]; $Q = AV$ represents the hydrological flux [m^3/s]; g is gravitational acceleration [m/s^2]; s_0 is the bottom slope of the pipeline [m/m]; s_f is the loss of friction resistance per unit length of pipeline [m/m]; and h_L is the loss of local resistance per unit length of pipeline [m/m].

2.2 Coupling of hydraulic models

As mentioned above, ANUGA can powerfully simulate overland water flow processes, and SWMM uses the full 1D Saint-Venant equations to compute the water flow in a sewer system (Martins et al., 2018). However, for surface flows, a nonlinear reservoir model is used to consider

other surface hydrological processes. The heterogeneities of features are considered for parameters in each subcatchment, such as the proportions of pervious and impervious areas, to consider different types of land features (Sharifan et al., 2010; Bisht, et al., 2016). SWMM cannot simulate the overland flow processes in detail. Therefore, the coupling of these two models can be helpful to simulate the overland/sewer system flow processes in an integrated way.

2.2.1 Modelling of the bi-directional interactions between overland flow and sewer flow

Artificial sewer systems are important infrastructures in PFF simulations, so simulations considering heterogeneity should support the bi-directional interactions between overland flow and the sewer system. The bi-directional interactions include the vertical flow interactions at manholes and outfalls, where the water height at the surface is H_{Surf} and the water height at the manhole is H_{Mhole}. Therefore, the bi-directional interaction scenarios are as follows: (1) when $H_{Mhole}<H_{Surf}$, the capacity of the sewer system can fully handle the inflow, the manholes do not experience overflow, and overland flow enters the sewer system through the manholes; (2) when $H_{Mhole}\geq H_{Surf}$, the capacity of the sewer system cannot cope with the inflow, and some overflow from manholes occurs; and (3) in other cases, water naturally flows from the outfalls. Scenarios (2) and (3) can be considered one type of water interaction. The flow scenarios involving bi-directional interactions are shown in Figure 1.

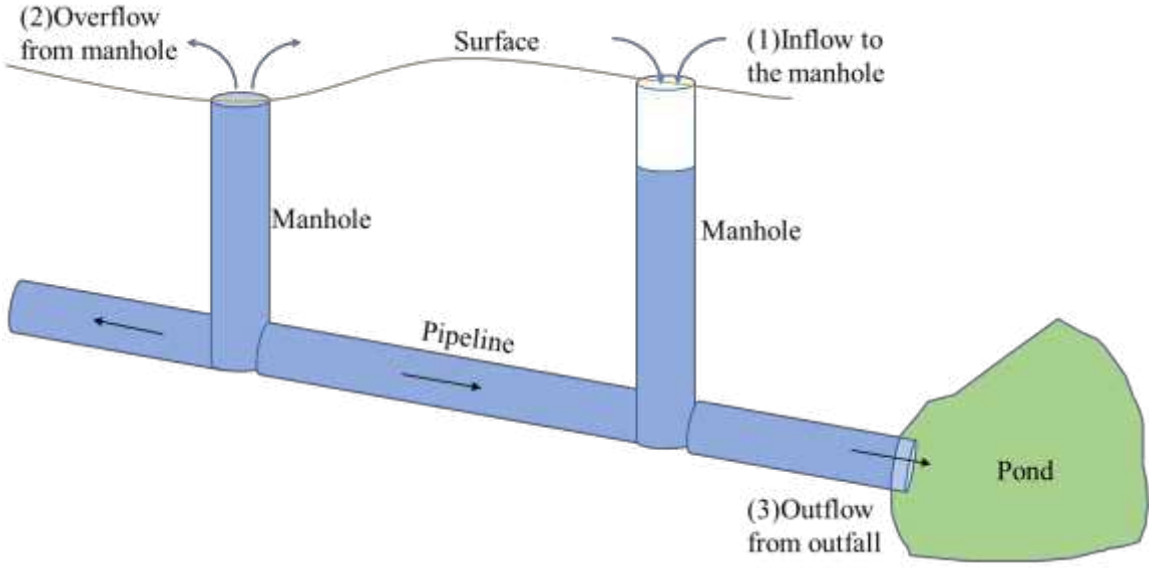

Figure 1. The scenarios of flow processes with bi-directional interactions

(1) Interactions between overland water flow and sewer system flow through manholes

a. Computation of the volume of inflow to manholes

The process of overland water flow into a sewer system may manifest two scenarios: (1) the manhole and related pipelines have enough space to receive the related water from the surface, and all the surface water can flow into the sewer system; or (2) the manhole and related pipelines contain some water, and none of the water in the corresponding areas can flow into the sewer system. The first situation can be analysed according to the water depths in the corresponding simulation steps and the areas of the corresponding manhole entrances, and the corresponding inflow volume equation can be expressed as $Q_s = A_m \bullet h/\Delta t$, where Q_s represents the inflow to the manhole [m^3/s], A_m is the manhole area, and h is the surface water depth in the corresponding manhole area. In the second situation, the water in the corresponding areas cannot flow into the manhole completely, but some water can flow into the sewer system through the manhole. The amount of water that can flow into the manhole is based on the status of the corresponding manhole and downstream pipelines. The volume calculation equation for the second situation can be expressed as $Q_s = (A_m \bullet h_m + A_p \bullet l_p \bullet k_p)/\Delta t$, where A_m is the area of the manhole cross section [m^2], h_m is the empty depth of the manhole [m], A_p is the area of the cross section of the related downstream pipeline [m], l_p is the length of the related pipeline [m], and k_p is the fullness ratio of the pipeline.

b. The correction of the source terms in the shallow water equation

For the outflow water that flows into the manhole from the ground, the shallow water equation should be subtracted from the source terms. The source term correction can be expressed as follows:

$$S = \begin{bmatrix} Q_R \pm q_S \\ gh(S_{0_x} - S_{f_x}) \\ gh(S_{0_y} - S_{f_y}) \end{bmatrix} + \begin{bmatrix} 0 \\ ghS_{b_x} \\ ghS_{b_y} \end{bmatrix} \quad (5)$$

where Q_R is the rainfall per unit time and unit area [m/s]; q_S represents the volume of outflow or the volume of the inflow per unit area and unit time [m/s], where an inflow is represented by a plus sign an outflow is represented by a negative sign; S_0 is the slope of the bottom; S_{b_x} is the effect of barriers; S_f is the friction of the bottom; g is gravitational acceleration; and h is the water depth. The flow charts of outflow and inflow for the manhole are shown in Figure 2.

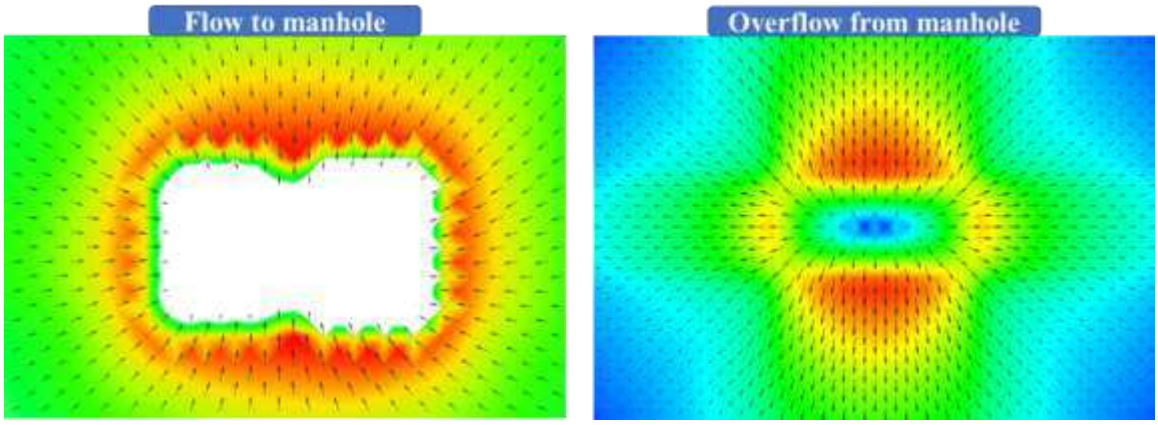

Figure 2. Flow charts of outflow and inflow for the manhole

2.2.2 The roof water flow into the sewer system

The heterogeneity of roofs and sewer systems results in extremely complex interactions among roofs, sewer systems, and the surface. This paper generalizes these heterogeneities into two types: (1) if a building contains or is associated with manholes, water flows directly from the roof into the manholes, and (2) if the building does not contain or is not associated with a manhole, the water from the roof is directly distributed at the surface. If a roof contains green infrastructure, this feature should also be considered. The first situation is based on the topographic relationships between the footprints of buildings and manholes. The flux at each manhole is the same in each simulation step, and the calculation of the flux is based on the average value according to the number of manholes and the area of the roof. A basic calculation is shown in Figure 2(1). Taking the building in 2(1) as an example, the roof area is 6737 m^2, and the building is associated with 25 manholes, so each manhole can hold 269.6 m^2 of water. In the second situation, the building does not contain any manholes or sewer nodes, so the water on the roof flows to the adjacent surface. Although the footprints of buildings are typically complex and irregular, this article simply considers the footprints of buildings to be rectangular. The basic calculation is shown in Figure 2(2). In this case, the building does not have any associated manholes, so the water flows directly to the surface. The building is generalized with four edges, and each edge has a given flux of water based on the corresponding length ratio considering the full length of the building outline. The roof water distribution rules are shown in Figure 3.

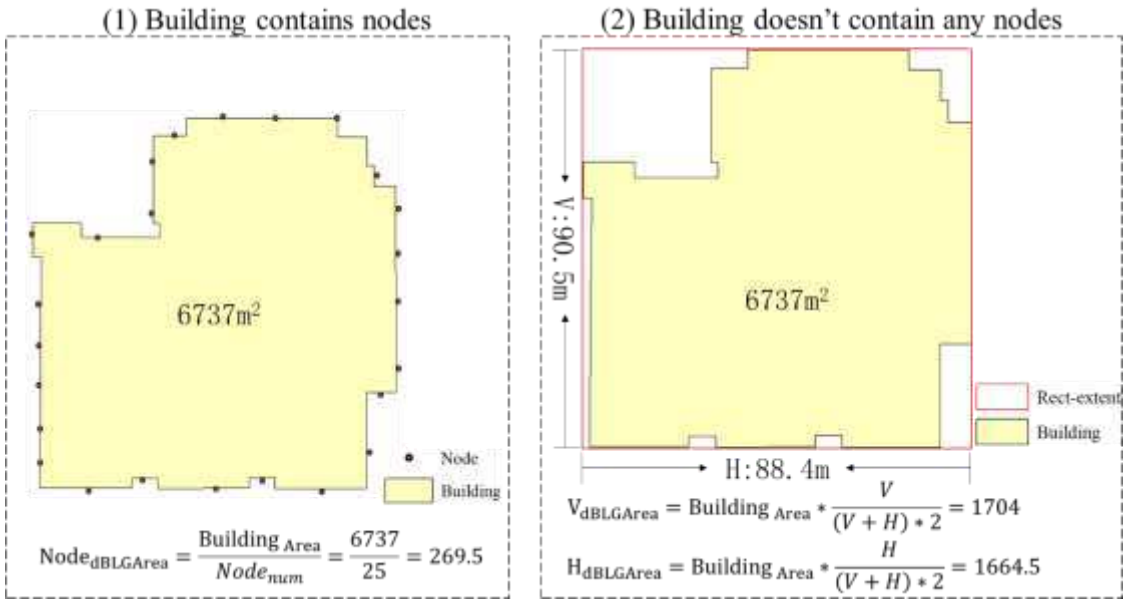

Figure 3. The roof water distribution rules

The flux for each manhole and edge is calculated by the equation $Q_{MBlg} = Q_R \bullet \text{Node}_{\text{ABlg}}$, where Q_{MBlg} represents the flux flow into the manhole from the roof or the flux that is distributed to the adjacent edge in the simulation step, Q_R represents the rainfall in the simulation step, and $\text{Node}_{\text{ABlg}}$ represents the drainage area of the manhole or edge.

2.2.3 Integration with the infiltration model

ANUGA does not include an infiltration model for water infiltration computations. With the advantages of obtaining the input parameters, the Horton infiltration model is used to calculate the water infiltration processes for different types of surfaces (Bauer, S. W. ,1974). The method of correction of the source terms in the shallow water equation is used to integrate the infiltration model. The corresponding source codes of ANUGA are also modified.

2.3 Coupling of the ANUGA and SWMM model systems

ANUGA and SWMM are two different model systems, so some specific technical strategies are used to implement the coupled simulation based on these two models.

2.3.1 Encapsulation and calling of SWMM

The computation programmes of overland flow processes in SWMM were substituted by ANUGA. A rainstorm event influences the surface first; therefore, this article uses ANUGA as the main loop control programme. SWMM is encapsulated as a Dynamic Link Library (DLL), and some interfaces are developed used to be called by ANUGA. The coupled simulation uses the

Ctypes module in Python to conduct the data exchange between the two models. The encapsulation of SWMM in ANUGA and calling of SWMM functions involve 4 steps: (1) the extraction of the EXTRAN module from SWMM and implementation of the *swmm_FlowExchange* interface for the flux exchange between ANUGA and SWMM; this exchange flux includes the flux into the sewer system through manholes, the overflow from manholes, and the outflow from outfalls; (2) encapsulating and exporting the main operation functions in SWMM, e.g., swmm_Open(inpFile, rptFile, outFile), swmm_FlowExchange(lstQin, lstQout, lstNodeDepth), swmm_Step(), swmm_Start(int), swmm_End(), swmm_Report(), and swmm_Close(), which are essential functions used for different simulation processes in SWMM; (3) the *LoadLibrary* function in the *Ctypes* module of ANUGA is used to call the DLL exported in step (2), and some specific data exchange formats (e.g., *c_float* and *c_double*) are used to support the flux exchange functions in ANUGA; and (4) the SWMM data are loaded and initialized in ANUGA, and the simulation functions are based on the processes in SWMM. The basic processes are shown in Figure 4.

Figure 4. The basic processes of encapsulating SWMM in ANUGA

2.3.2 The implementation of inflow and outflow operators

ANUGA has a very specific programming framework for the model system. In this system framework, a shallow water equation-based computational engine is implemented as the core module, and the interactions among heterogeneous objects are considered using customizable operators and structurers. Therefore, the core of the ANUGA can maintain stability, and the surface features and corresponding mechanisms are independently considered based on procedural operators and structures. These operators and structures are customizable programming objects that are used to perform simulations and determine how specific heterogeneous objects, such as culverts and gates, affect overland flow.

This paper follows the basic rules of the programming framework in ANUGA, and two procedural operators, *manholein_operator* and *manholeout_operator*, are developed. These operators are used to model flows from the surface into manholes and overflows from manholes or outflows from outfalls. The main input parameters for *manholein_operator* include the centre

coordinates of the manhole, the length of the manhole, and the width of the manhole. The parameters for *manholeout_operator* include the outflow flow (Q) and the border of the manhole. Additionally, these two procedural objects include the interface *set_workStatus(bool)*, which is used to control the work status of operators. For example, when a manhole overflows, the manhole should no longer support inflow, and when the manhole stops overflowing, *manholeout_operator* should stop working. In this paper, each manhole is considered a specific procedural object, and the operator work status control interface can effectively manage these procedural objects. To efficiently manage computational resources, each manhole has a corresponding *manholein_operator,* which is initialized at the initial process of model simulation. However, the *manholeout_operator* objects are dynamically added when overflow occurs at the manhole.

2.3.3 The processes of the ANUGA main loop control-based bi-directional simulation

The data preprocessing and initialization steps are completed before the main loop involving water flow calculations. The water interactions between the two models are considered at each simulation step. The basic simulation processes are as follows.

a. Load the simulation scenario to obtain the configuration information and essential input data for the simulation, which mainly include discretized cells, the extent of the simulation area, and the sewer system data.

b. Set the initial parameters, such as the Manning coefficients for different types of mesh grids and land use types, as well as precipitation parameters.

c. Set the boundary conditions, which are used to define the water flow rules at the borders of the simulation area. The Dirichlet boundary condition supports flows out of the border, and the reflective boundary condition yields a solid boundary.

d. Initialize and start the SWMM model. In this step, ANUGA calls the SWMM operational interface.

e. Initialize the inflow and outflow procedural operators in terms of handling the inflow to manholes, overflow from manholes, and outflow from outfalls.

f. The overland flow, sewer flow, and corresponding interactions are modelled in the main loop programmes. The main steps in the loop are as follows: (1) performing the ANUGA-based overland flow calculation, which simulates the velocity, volume, and direction of overland flow at each simulation step; (2) executing the list of manhole-based loops, which is used to obtain the

283 volume of flow into each manhole at each simulation step; (3) calling the water flow exchange
284 interface, which sets the inflow volume for each manhole, and obtain the volume of overflow for
285 each manhole and the volume of outflow for each outfall; (4) calling the simulation step execution
286 function used to execute the steps in SWMM, where the simulation step in SWMM is the same as
287 that in ANUGA; (5) executing the list of manhole-based loops, which are used to handle the
288 overflow from manholes and dynamically add new procedural operators for the new flowing
289 manholes; (6) updating the volumes of overflows and outflows for the corresponding procedural
290 operators, which are added to the list of overflow nodes; and (7) outputting the ANUGA simulation
291 results into output files, which include the water depth, volume, velocity, and volumes for different
292 type of features.
293 g. Use the corresponding interfaces to end the simulation, and save the simulation results from
294 SWMM.
295 h. Finish the coupled simulation, and save the simulation logs.
296 The workflow for the coupled simulation is shown in Figure 5.

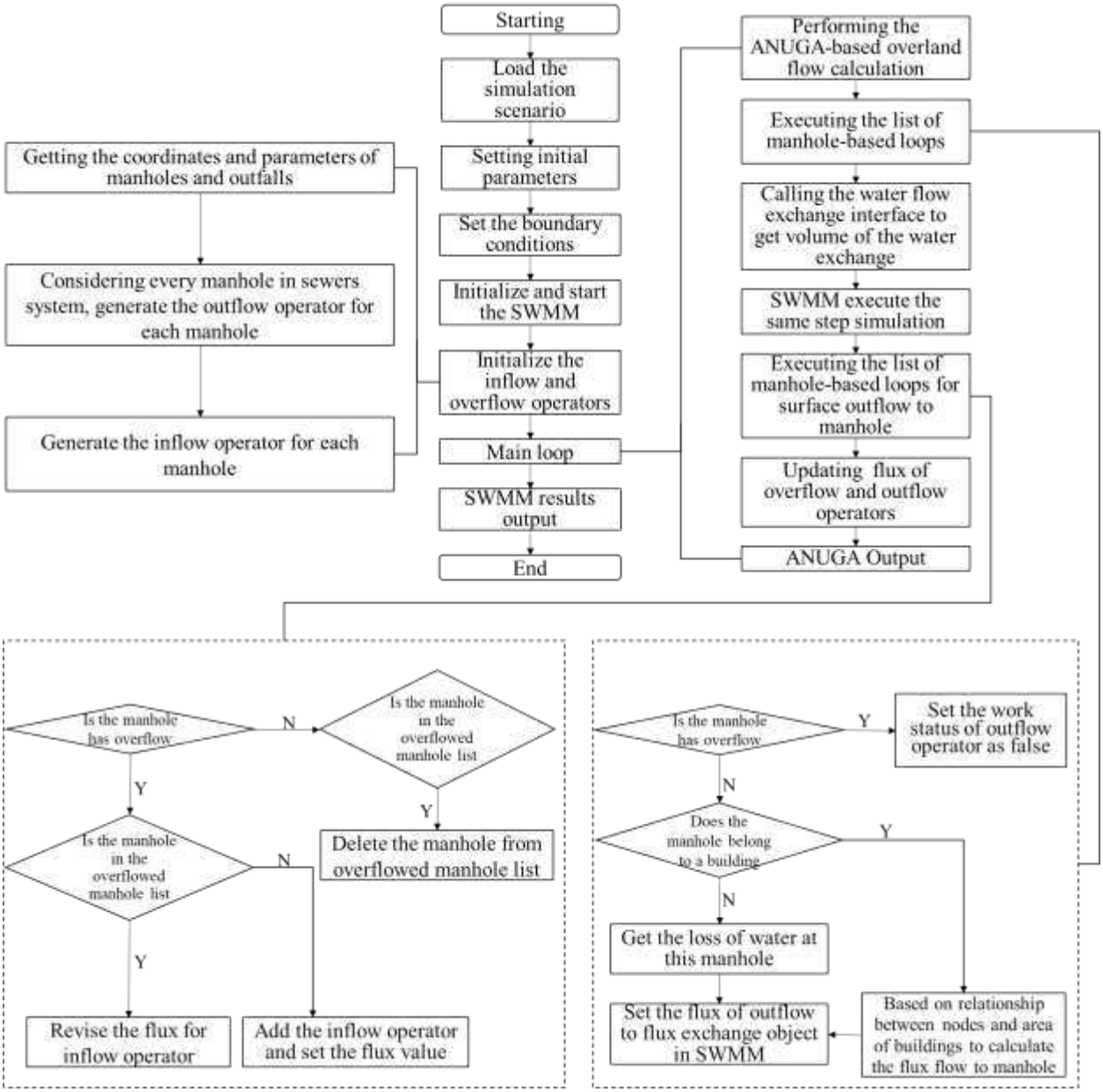

Figure 5. The workflow for the coupled simulation

3. Case study description

3.1 Study area and data

This article used a university campus as the research area. This area is located in the northeast portion of Nanjing city in Jiangsu Province. Jiangsu is an east-central coastal province in China. The topography of the research area mainly includes hills and plains, and the hills are located in the northern part of the plain area, forming a half-surrounded topographic area. Thus, this research

area has an obvious advantage in setting boundary conditions. The topography decreases progressively from the north to the south, so the research area is rarely impacted by exterior inflows from adjacent regions. The basic GIS data for the surface include digital elevation model (DEM and road network, building, and land use type data. The sewer data include manhole, pipeline, and outfall information. The types of manholes are rainwater inlets, rainwater grates, catch basins, and valves. To fully consider the heterogeneity of this urban area, this article uses high-resolution data, and most of these data were acquired from the official agency of surveying. The resolution of the DEM is 1 metre in each cell, and the scales of buildings, land use, and water bodies are 1:1000. The vector layer of roads was vectorized based on a 1:500 scale map. The location of the study area and the basic data are shown in Figure 6.

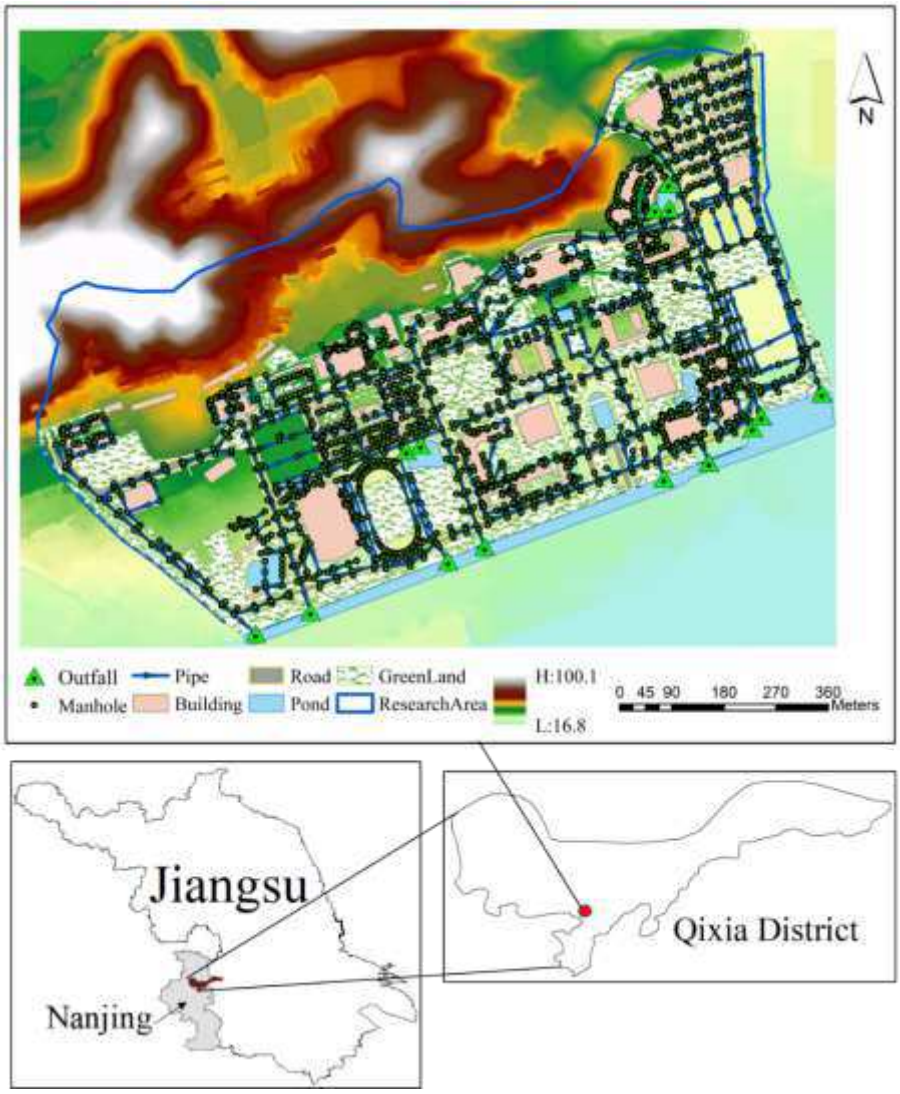

Figure 6. The location of the study area and the basic data

3.2 Rainstorm events

The experiment in this study was based on a rainstorm event that occurred on 2016/07/01. During the 12-hour precipitation period on that day, the peak precipitation occurred between 6:00 am and 8:00 am, and 55.9 mm precipitation fell in these two hours in the research area. The rainfall time series is shown in Figure 7. To improve the experimental efficiency, the experiment used only two hours of precipitation as the simulation time. Before that, almost 8 mm precipitation occurred over 10 h, and we considered this 8 mm precipitation as the initial loss in SWMM.

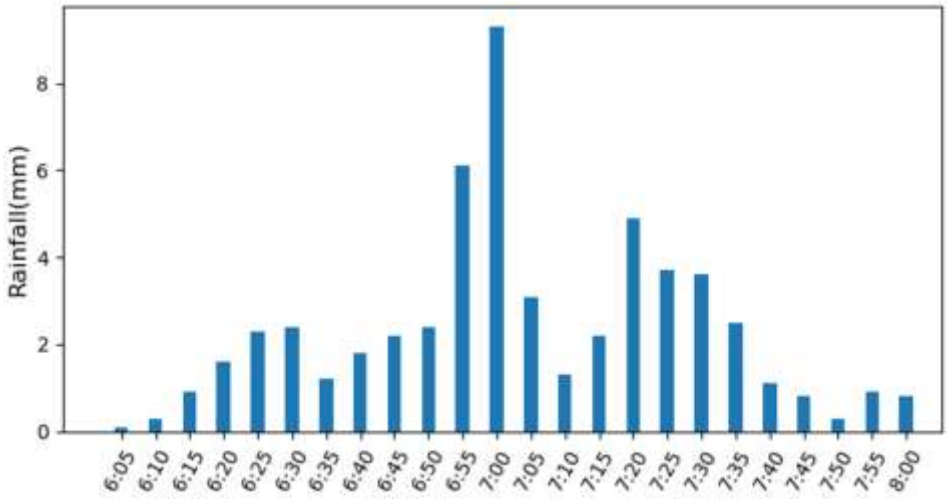

Figure 7. The rainfall time series of the storm event

4. Experiment

4.1 Boundary conditions and parameter setting

This paper used a Dirichlet boundary (the overland flow continues out of the research area from the boundary) to consider the outflow from the research area. A reflective boundary (momentum vector reflected 180 degrees from the footprints of buildings) was used for the building footprints, and the footprints were discretized as interior holes in this experiment. Additionally, to optimally consider the integral flux in the research area, a hydrological basin that enveloped the campus area was created. The set of boundary conditions is shown in Figure 8.

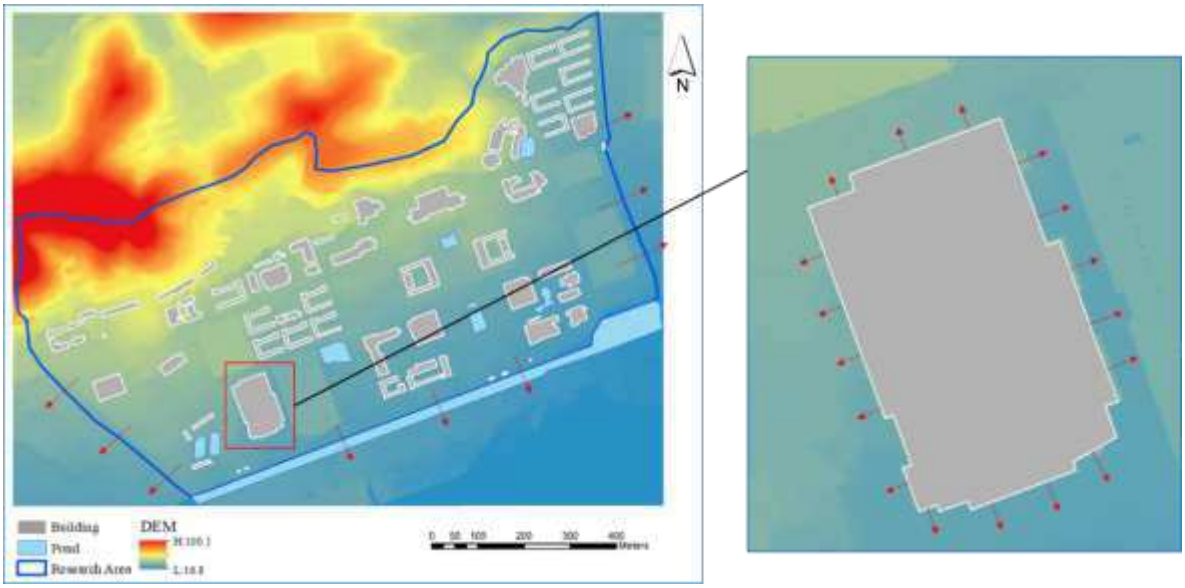

Figure 8. The boundary conditions

4.2 Spatial discretization and sewer data translation

Because the heterogeneity of the research area can be expressed in the model simulation process, this article uses the original surveying data to conduct spatial discretization. Spatial discretization is the bridge that connects the real world and simulation-based computations. According to the specific computational methods, the heterogeneous characteristics of the surface were discretized into the corresponding scheme used to support the model simulation. The topographic characteristics of the surface were fitted to the discretized mesh cells. The buildings were considered as interior holes, and the precipitation that fell on buildings flowed into manholes based on the average distribution. This article does not consider the timing of this water flow process from building roofs to sewer systems or surfaces. These manholes are encompassed by or touch the corresponding building borders. The surface of roads is usually 15 cm-25 cm lower than the edges of roads. Therefore, roads usually have obvious water confluence effects, forming flow channels. Additionally, many manholes are located along roads, and the accuracy of water flow simulations on roads notably impacts PFF modelling. Therefore, this article also considers the concavity of roads based on the original DEM data interactions. Fig. 9(A) illustrates the discretization of the main heterogeneous objects associated with the urban surface. Fig. 9(B) shows the data preprocessing step for the sewer system, in which the sewer data are discretized from GIS vector data format into an SWMM-supported format.

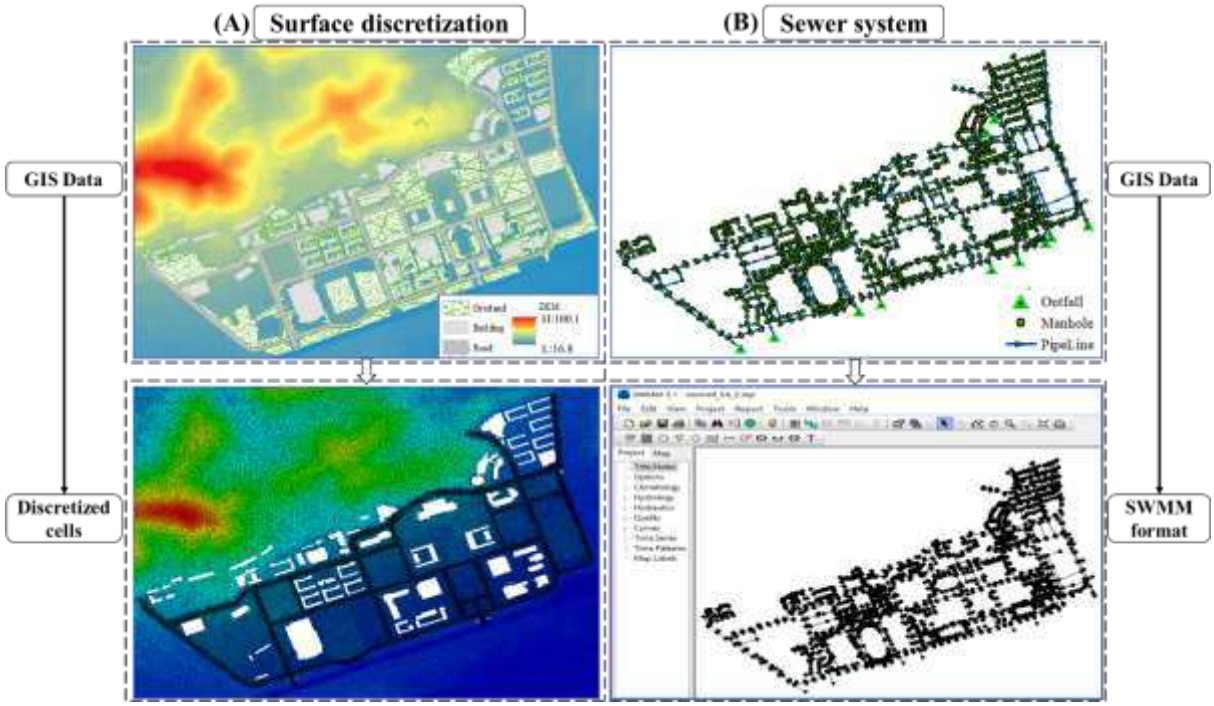

Figure 9. Spatial discretization and data transformation

4.3 Parameter setting

The parameters for ANUGA and SWMM include the Manning coefficient for different types of surfaces, the Manning coefficient for pipelines, and the parameters for the Horton infiltration model. The parameters for the simulation proposed in this article are based on references of similar research cases. The parameters are shown in Table 3. To reduce the continuity error in SWMM, this article uses 1 second as the simulation step for SWMM and ANUGA. The calculation of water transport in the sewer system is based on the dynamic wave model.

Table 3. The parameters of the integrated model

Parameter	Type	Value	Unit
Manning's n value	Permeable area	0.12	$s/m^{1/3}$
	Impermeable area	0.015	$s/m^{1/3}$
	Pipe	0.019	$s/m^{1/3}$
	River/Pond	0.02	$s/m^{1/3}$
Horton infiltration parameters	Minimum rate	30.5	mm/h
	Maximum rate	77.5	mm/h
	Decay constant	3.78	1/h

5. Results and discussion

5.1 The validation of water-logged locations

The validation of water-logged locations in this experiment is shown in Fig. 10. Due to the advantages of the local topography and the water drainage ability of the sewer system in the research area, large flooding did not occur, and only two water-logged sites were observed. Locations A and B are water-logged areas, and locations C, D, E, F, G, and H are swimming pools and landscape ponds on the campus. A comparative analysis of locations A and B indicates that the simulation results accurately identified the actual water-logged locations. Because the actual flood areas change dynamically, the real flood areas are very small in this storm event (e.g., the road width of location A is approximately 4.5 m), and it is difficult to identify the real border of the flood area by photos. Approximately, for location A, the prediction of the flooded surface area was 51% of the actual surface area; for location B, the prediction of the flooded surface area was 62% of the actual surface area. Additionally, a comparative analysis of the other six locations (locations C-H) marked on the map indicated that the borders of these areas were accurately simulated. The border of a pool or pond is an important heterogeneous characteristic, and the simulation results for pool areas verified the capabilities of the simulation model. The validation of water-logged locations is shown in Figure 10.

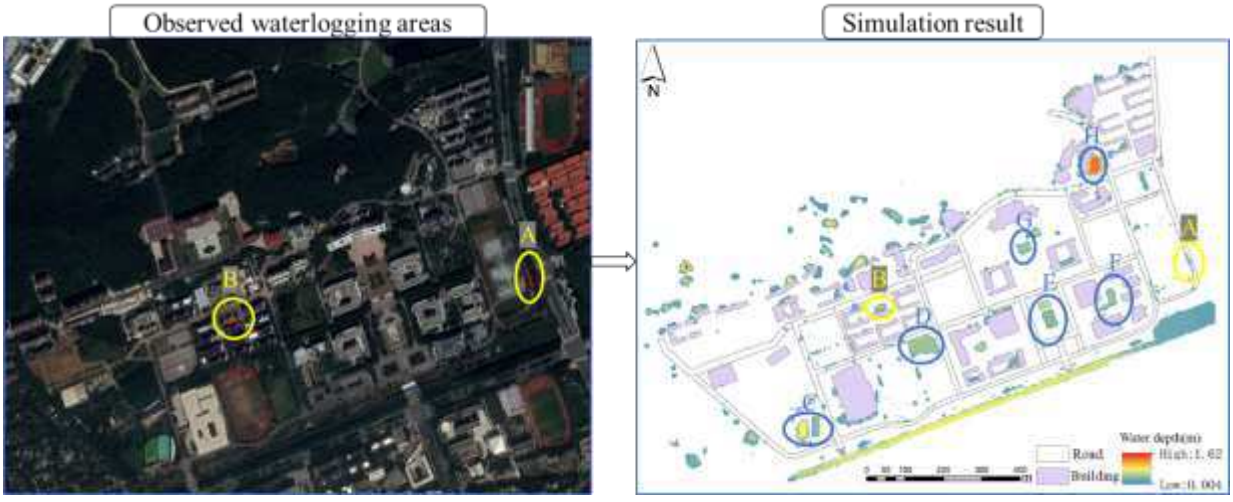

Figure 10. The validation of water-logged locations

5.2 Analysis of the heterogeneous feature-based simulation results

(1) Analysis of overflow nodes

In this simulation, only nodes 5Y386 and 3Y688 experienced overflow, and the total overflow volume was 4.5804 m^3. The overflow volume of node 5Y386 was 4.58 m^3, and the overflow volume of node 3Y688 was 0.0004 m^3. The locations of the two overflow nodes and the upstream and downstream relationships are shown in Figure 11. The main reason that node 5Y386 appeared to overflow was related to the source data. Node 5Y386 was designed as the terminal downstream node, so a large volume of water flows to this node.

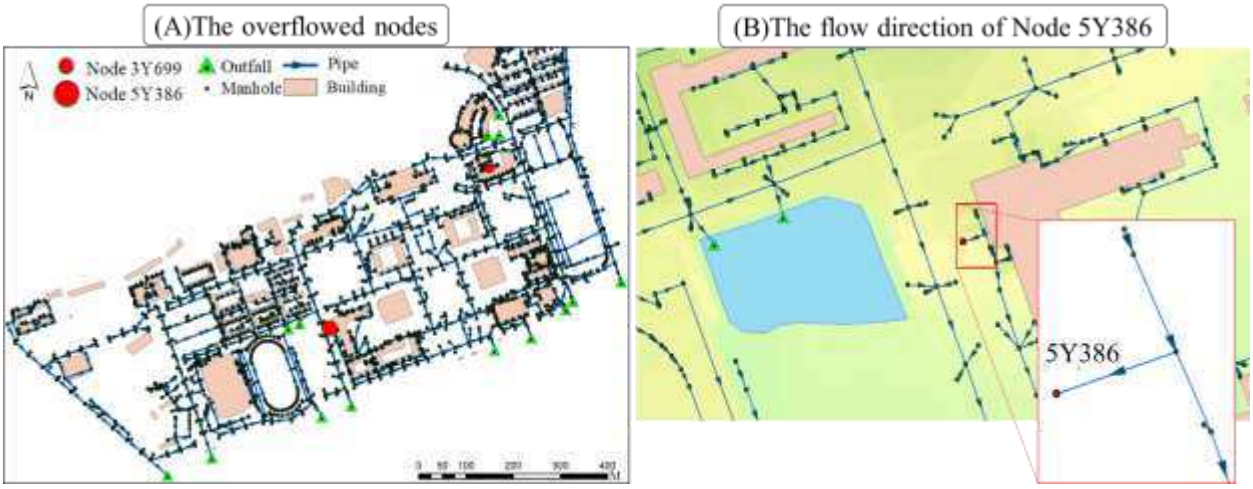

Figure 11. The overflowed nodes and topological relationships

(2) The volumes for different processes

In this simulation, the total volume flowing into the sewer system through the manholes was 23712.49 m^3, the volume flowing into the sewer system from the surface was 19254.04 m^3, and the volume flowing into the sewer system from buildings was 4458.45 m^3. The total outflow volume from outfalls was 23272.14 m^3, the outflow volume that flowed into pools was 4722.48 m^3, and the total infiltration volume was 13241.17 m^3. Therefore, it is estimated that almost 3175.92 m^3 of water flowed outside of the research area on the surface. However, the volume of outflows from the surface did not include the overlap of water volumes transported among various nodes, surface channels and pools. The water volumes from different sources flowing into the sewer system are shown in Table 4.

Table 4. The water volumes from different sources flowing into the sewer system

Flow type	Total flow into the sewer	Flow into the sewer through the surface	Flow into the sewer through the building	Total outflow from outfalls	Outflows to lakes	Infiltration flow	Overflow volume
Flux (m^3)	23712.49	19254.04	4458.45	23272.14	4722.48	13241.17	4.58

(3) The water volumes of flow processes

The time series of surface runoff and the volume of pools are shown in Figure 12. The time series of surface runoff is highly similar to the rainfall time series. Due to the accumulation of surface flow, the peak surface runoff occurred at 1 h 33 min or at the 5580th simulation step. The peak volume of pools occurred at the end time of the simulation, which suggests that the volume of pools continued to increase until the end of the simulation, but the rate of increase slowed over time.

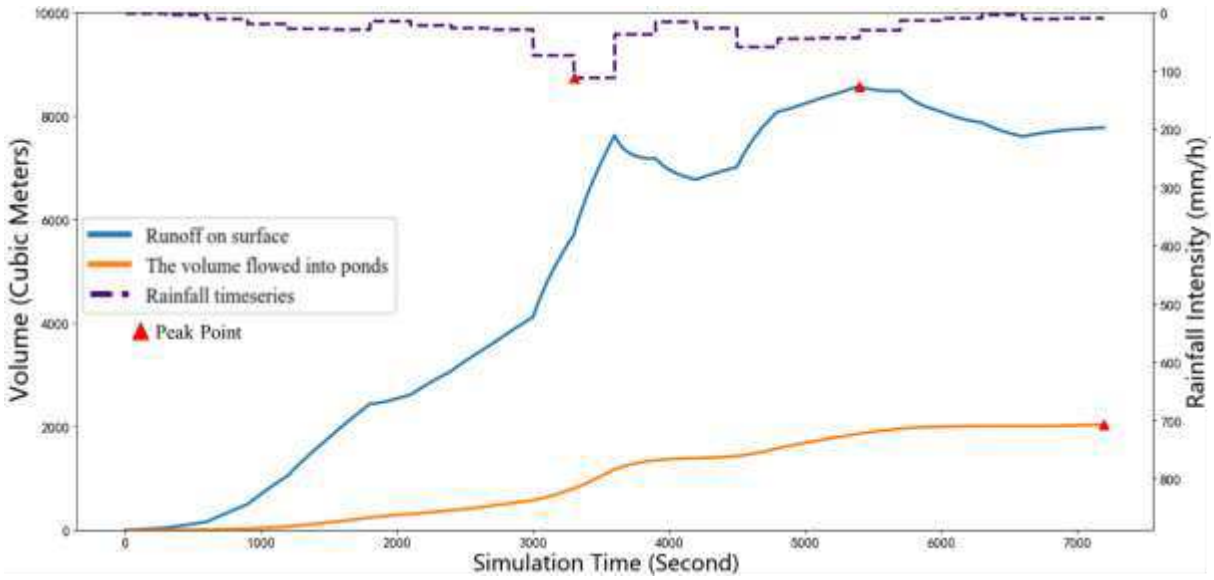

Figure 12. The time series of surface runoff and the volume of pools

In this simulation, the water-logged areas are shallow water areas, and the intensity of water flow is very low in most areas. The highest water flows occurred at the outfalls, as shown by the flow field in Figure 13. The simulation step depicted in Figure 15 is the 3710th; at this step, the volume at outfall 3Y120 is 1.209 m^3, the volume at outfall 3Y107 is 1.02 m^3, and the volume at outfall 3Y0890 is 0.104 m^3. Because fewer upstream nodes and areas are drained by outfall 3Y0890 compared to those for outfalls 3Y120 and 3Y107, the water volume at 3Y0890 is also lower than those at the other two outfalls.

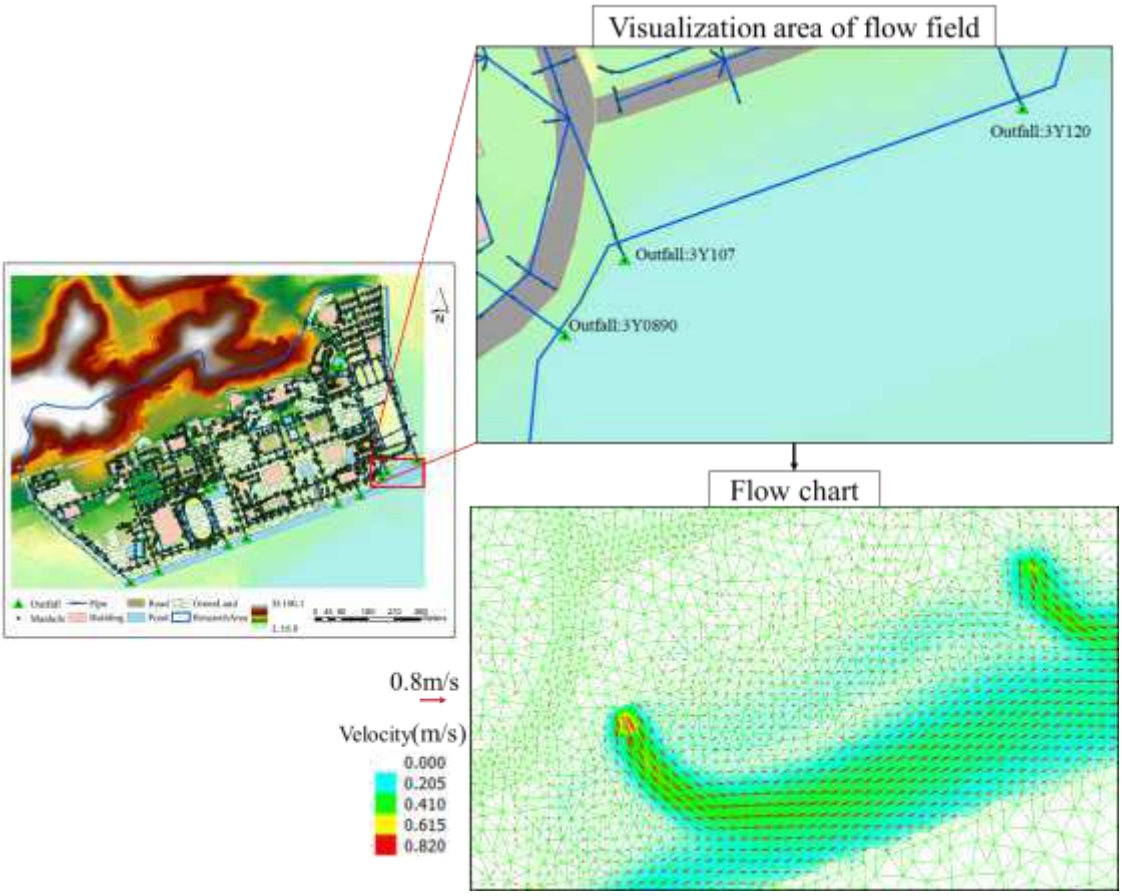

Figure 13. The analysis of the intensity of overland flow

5.3 Comparative analysis of the simulation results based on different models

A comparative analysis based on SWMM, ANUGA, and the coupled model proposed in this article was performed to analyse the differences among the simulation results from the aspect of heterogeneity. The time period of the simulation step in the 3 models was the same and set to 1 second. Automatic topographical analysis algorithms and manual processing were used to divide catchments. The parameters for SWMM were as follows: the Manning coefficient for pervious areas was 0.9; the Manning coefficient for impervious areas was 0.008; the water storage depth in impervious depression areas was 4 mm; the water storage depth in pervious depression areas was 6 mm; the Manning coefficient for pipes was 0.013; the loss coefficient for pipes was 0.2; the Manning coefficient for culverts and pools was 0.025; the maximum rate of Horton infiltration was 75.5 (mm/h); the minimum rate of Horton infiltration was 3.5 (mm/h); and the decay constant in the Horton infiltration model was 3 (1/h). Additionally, to reduce the impacts caused by the discretization of cells, ANUGA and the proposed coupled model used the same discretization resolution. The simulation results for the three models are shown in Fig. 14.

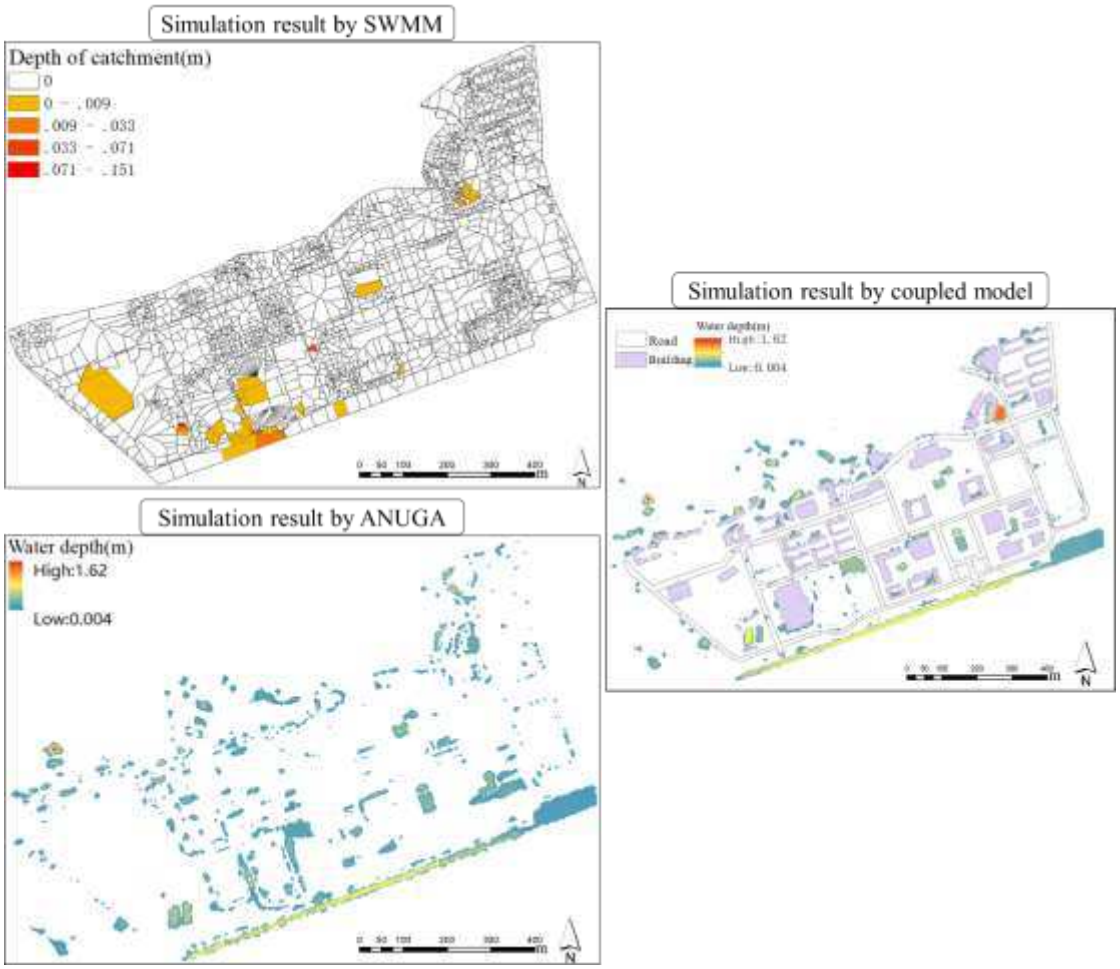

Figure 14. Comparative analysis based on SWMM, ANUGA and the integrated model

As shown in Figure 14, the simulation results from the proposed model could be more accurate in depicting water-logged areas, such as the outfalls of ponds, and changes in the water depth of pools. By considering the borders of features based on the developed spatial discretization programs, the water-logged areas near the borders of roads and water collection in pools are accurately depicted. Because of the catchment-based spatial discretization, the stand-alone SWMM model has difficulty depicting the heterogeneity of water-logged areas at the surface. SWMM can support sewer system planning, but it does not meet the needs of PPF simulations. Additionally, the stand-alone ANUGA model does not consider the interactions between overland flow and sewer system flow.

6. Conclusions and future work

This article combined two popular open-source models, SWMM and ANUGA, for the bi-directional coupling of overland flow and sewer system flow processes. Furthermore, this article is based on a coupled model and a spatial discretization method, which are used to conduct heterogeneous feature-based urban flood modelling and simulations, accurately model water flow processes and provide effective results for urban flood management. The experimental results based on a real storm event in an urban area demonstrated that the integrated model can accurately simulate areas of surface water accumulation. A comparative analysis based on three different models indicated that the coupled hydraulic model most accurately depicted the motion states of flows and various flooding areas.

However, this research has some limitations. First, due to the lack of basic GIS data, this article did not consider the impacts of culverts located near building boundaries. Thus, considerable waterlogging occurred near or within the footprints of buildings. Second, the parameters of these models are referenced from related studies, and the article did not consider other methods of setting the parameters. Additionally, this article did not consider the uncertainty of modelling, which should be assessed to better understand and verify the simulation results. The model results of infiltration, runoff, and outflow were or only compared with each other, they were not validated by instruments.

Acknowledgements: This work was supported by the National Key R & D Program of China (Grant Nos. 2018YFB0505500, 2018YFB0505502).

Author Contributions: Guoqiang Peng and Zhiyao Song provided the initial idea for this study; Guoqiang Peng designed and performed the experiment; Guoqiang Peng and Zhuo Zhang analysed the results of the experiment; and Guoqiang Peng and Arif Masrur wrote the paper.

Data Availability Statement: This study used secured datasets, as described in the experimental section, collected from the Nanjing Research Institute of Surveying & Mapping (NRISM). By conforming to the data sharing and usage policies, the datasets used in this research can be obtained from the NRISM only.

Conflicts of Interest: The authors declare no conflicts of interest.

References

Bauer, S. W. (1974). A modified Horton equation for infiltration during intermittent rainfall. Hydrological Sciences Journal, 19(2), 219-225.

Bisht, D. S., Chatterjee, C., Kalakoti, S., Upadhyay, P., Sahoo, M., & Panda, A. (2016). Modeling urban floods and drainage using SWMM and MIKE URBAN: a case study. Natural Hazards, 84(2), 749-776.

Chang, T. J., Wang, C. H., & Chen, A. S. (2015). A novel approach to model dynamic flow interactions between storm sewer system and overland surface for different land covers in urban areas. *Journal of Hydrology*, *524*, 662-679.

Chen W, Huang G, Zhang H, et al. Urban inundation response to rainstorm patterns with a coupled hydrodynamic model: A case study in Haidian Island, China[J]. Journal of hydrology, 2018,564, 1022-1035.

Dey A K, Kamioka S. An integrated modeling approach to predict flooding on urban basin[J]. Water Science & Technology, 2007, 55(4):19-29.

Djordjević S, Prodanović D, Maksimović Č, et al. SIPSON–Simulation of Interaction between Pipe flow and Surface Overland flow in Networks[J]. Water Science and Technology,2005,52(5):275-83.

Gironás J, Roesner L A, Rossman L A, et al. A new applications manual for the Storm Water Management Model (SWMM)[J]. Environmental Modelling & Software, 2010, 25(6):813-814.

Goodchild, M. F. (2018). Reimagining the history of GIS. Annals of GIS, 24(1), 1-8.

Hassan, W. H., Nile, B. K., & Al-Masody, B. A. (2017). Study the climate change effect on storm drainage networks by storm water management model [SWMM].

Jiang, Y., Zevenbergen, C., & Fu, D. (2017). Understanding the challenges for the governance of China's "sponge cities" initiative to sustainably manage urban stormwater and flooding. Natural Hazards, 89(1), 521-529.

Leandro, J., Schumann, A., & Pfister, A. (2016). A step towards considering the spatial heterogeneity of urban key features in urban hydrology flood modelling. *Journal of Hydrology*, *535*, 356-365.

Lee, S., Nakagawa, H., Kawaike, K., & Zhang, H. (2016). Urban inundation simulation considering road network and building configurations. *Journal of Flood Risk Management*, *9*(3), 224-233.

Martins, R., Leandro, J., & Djordjević, S. (2018). Influence of sewer network models on urban flood damage assessment based on coupled 1D/2D models. Journal of Flood Risk Management, 11, S717-S728.

Mignot, E., Paquier, A., & Haider, S. (2006). Modeling floods in a dense urban area using 2D shallow water equations. Journal of Hydrology, 327(1-2), 186-199.

509 Mungkasi S, Roberts S G. Validation of ANUGA hydraulic model using exact solutions to shallow
510 water wave problems[J]. Journal of Physics: Conference Series, 2013, 423:12-29.
511 Mungkasi S, Roberts S. G, Davies, et al. Validations
512 report.https://github.com/GeoscienceAustralia/anuga_core/blob/master/doc/validations_report.pdf. 2015.
513 Nielsen O, Roberts S, Gray, D, et al. Hydrodymamic modelling of coastal inundation [J]. Austrailan
514 National University Open Research Library, 2005, 6(4):12-53.

515 Roberts S, Nielsen O, Gray D, et al. ANUGA user manual. Geoscience Australia. 2010. Available at
516 https://en.wikipedia.org/wiki/ANUGA_Hydro

517 Rossman L A. Storm water management model user's manual, version 5.0. 2010, Cincinnati:
518 National Risk Management Research Laboratory, Office of Research and Development, US Environmental
519 Protection Agency.

520 Sang, Y. F., & Yang, M. (2017). Urban waterlogs control in China: more effective strategies and
521 actions are needed. Natural Hazards, 85(2), 1291-1294.
522 Sharifan, R. A., Roshan, A., Aflatoni, M., Jahedi, A., & Zolghadr, M. (2010). Uncertainty and
523 sensitivity analysis of SWMM model in computation of manhole water depth and subcatchment peak flood.
524 Procedia-social and behavioral sciences, 2(6), 7739-7740.
525 Wang, D., Cao, W., Xin, X., Shao, Q., Brolly, M., Xiao, J., ... & Zhang, Y. (2017). Using vector
526 building maps to aid in generating seams for low-attitude aerial orthoimage mosaicking: Advantages in
527 avoiding the crossing of buildings. ISPRS Journal of Photogrammetry and Remote Sensing, 125, 207-224.
528 Wang, Y., Chen, A. S., Fu, G., Djordjević, S., Zhang, C., & Savić, D. A. (2018). An integrated
529 framework for high-resolution urban flood modelling considering multiple information sources and urban
530 features. Environmental modelling & software, 107, 85-95.
531 Wu, X., Wang, Z., Guo, S., Liao, W., Zeng, Z., & Chen, X. (2017). Scenario-based projections of
532 future urban inundation within a coupled hydrodynamic model framework: A case study in Dongguan City,
533 China. Journal of hydrology, 547, 428-442.

534 Wu X, Wang Z, Guo S, et al. A simplified approach for flood modeling in urban environments[J].
535 Hydrology Research,2018,49(6):1804-1816.
536 Xiao, Y., Yi, S., & Tang, Z. (2017). Integrated flood hazard assessment based on spatial ordered
537 weighted averaging method considering spatial heterogeneity of risk preference. Science of The Total
538 Environment, 599, 1034-1046.
539 Yang, Q., Dai, Q., Han, D., Zhu, X., & Zhang, S. (2018). Impact of the Storm Sewer Network
540 Complexity on Flood Simulations According to the Stroke Scaling Method. Water, 10(5), 645.

Yin, J., Yu, D., Yin, Z., Liu, M., & He, Q. (2016). Evaluating the impact and risk of pluvial flash flood on intra-urban road network: A case study in the city center of Shanghai, China. Journal of hydrology, 537, 138-145.

Zhang, H., Zhu, J., Xu, Z., Hu, Y., Wang, J., Yin, L., ... & Gong, J. (2016). A rule-based parametric modeling method of generating virtual environments for coupled systems in high-speed trains. Computers, Environment and Urban Systems, 56, 1-13.

Zoppou C, Roberts S. Catastrophic collapse of water supply reservoirs in urban areas[J]. Journal of Hydraulic Engineering, 1999, 125(7):686-695.

Figures

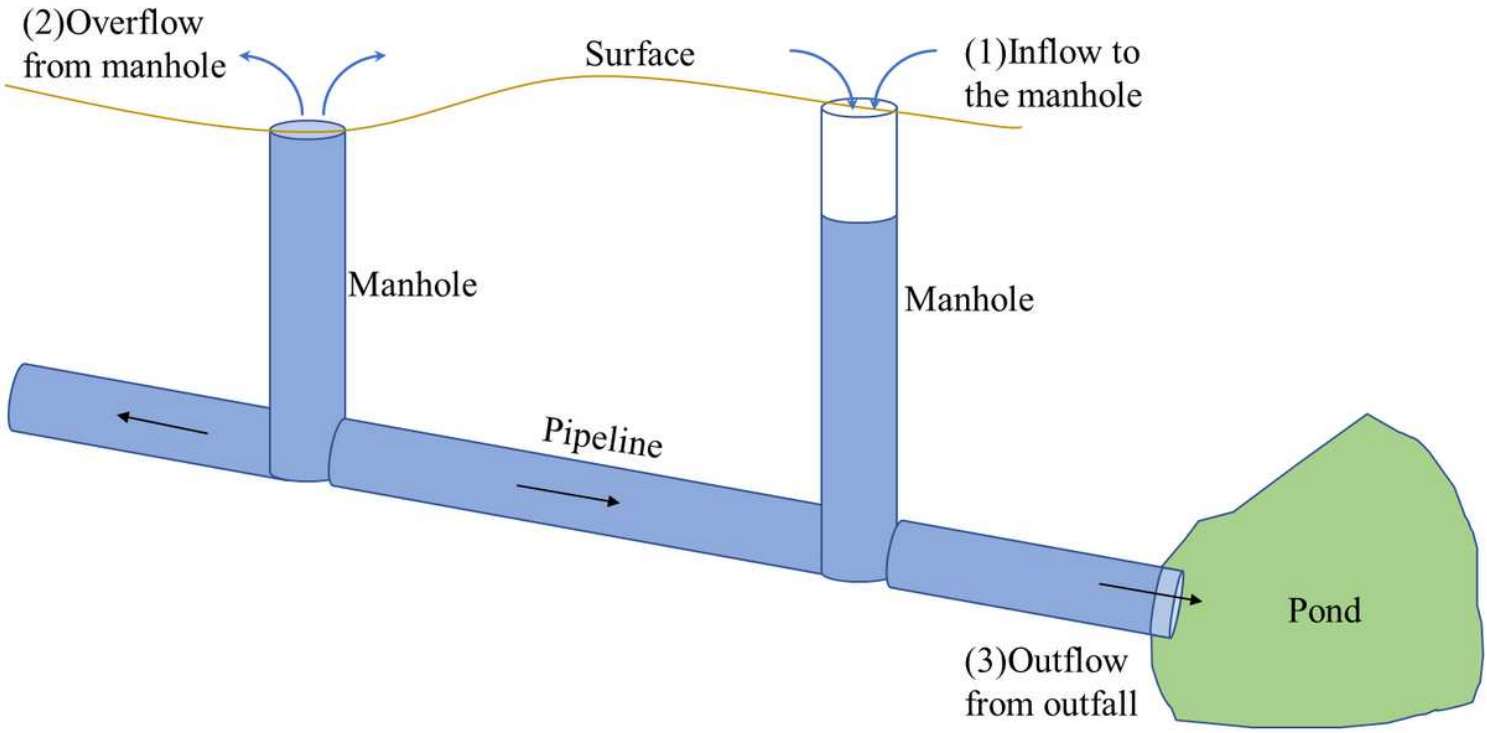

Figure 1

The scenarios of flow processes with bi-directional interactions

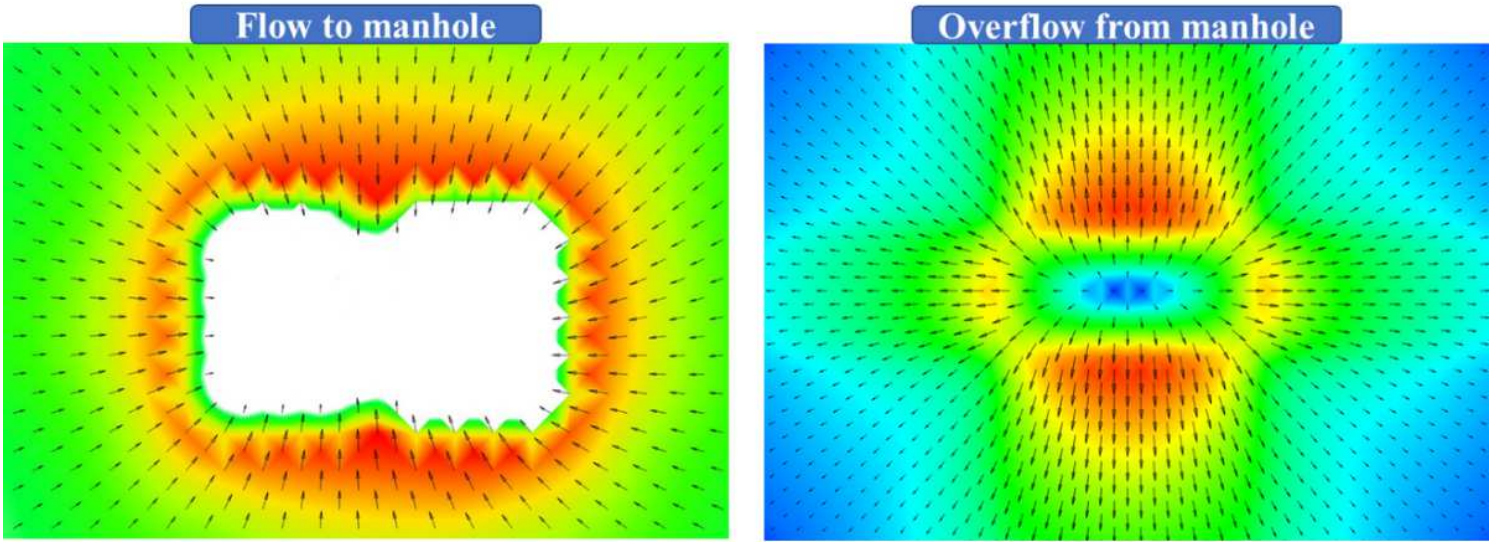

Figure 2

Flow charts of outflow and inflow for the manhole

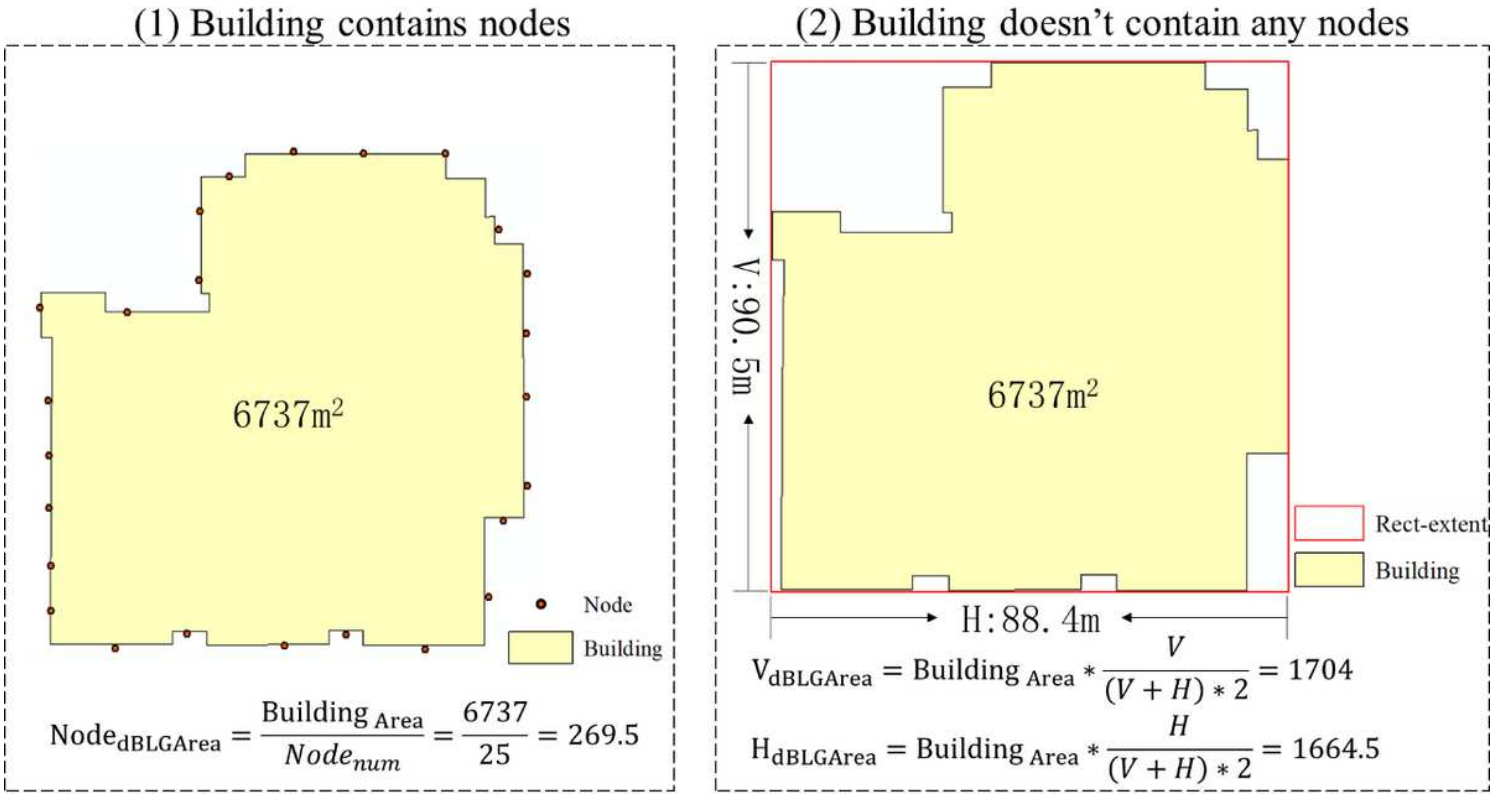

Figure 3

The roof water distribution rules

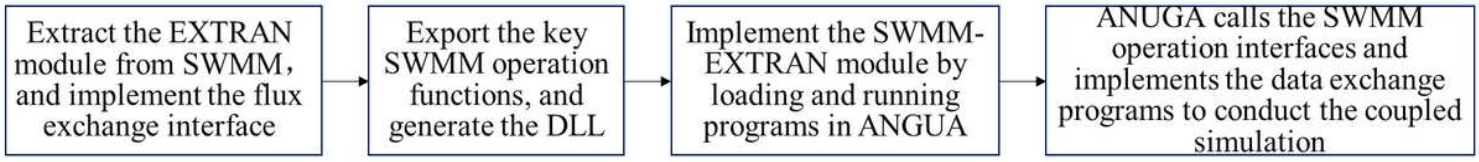

Figure 4

The basic processes of encapsulating SWMM in ANUGA

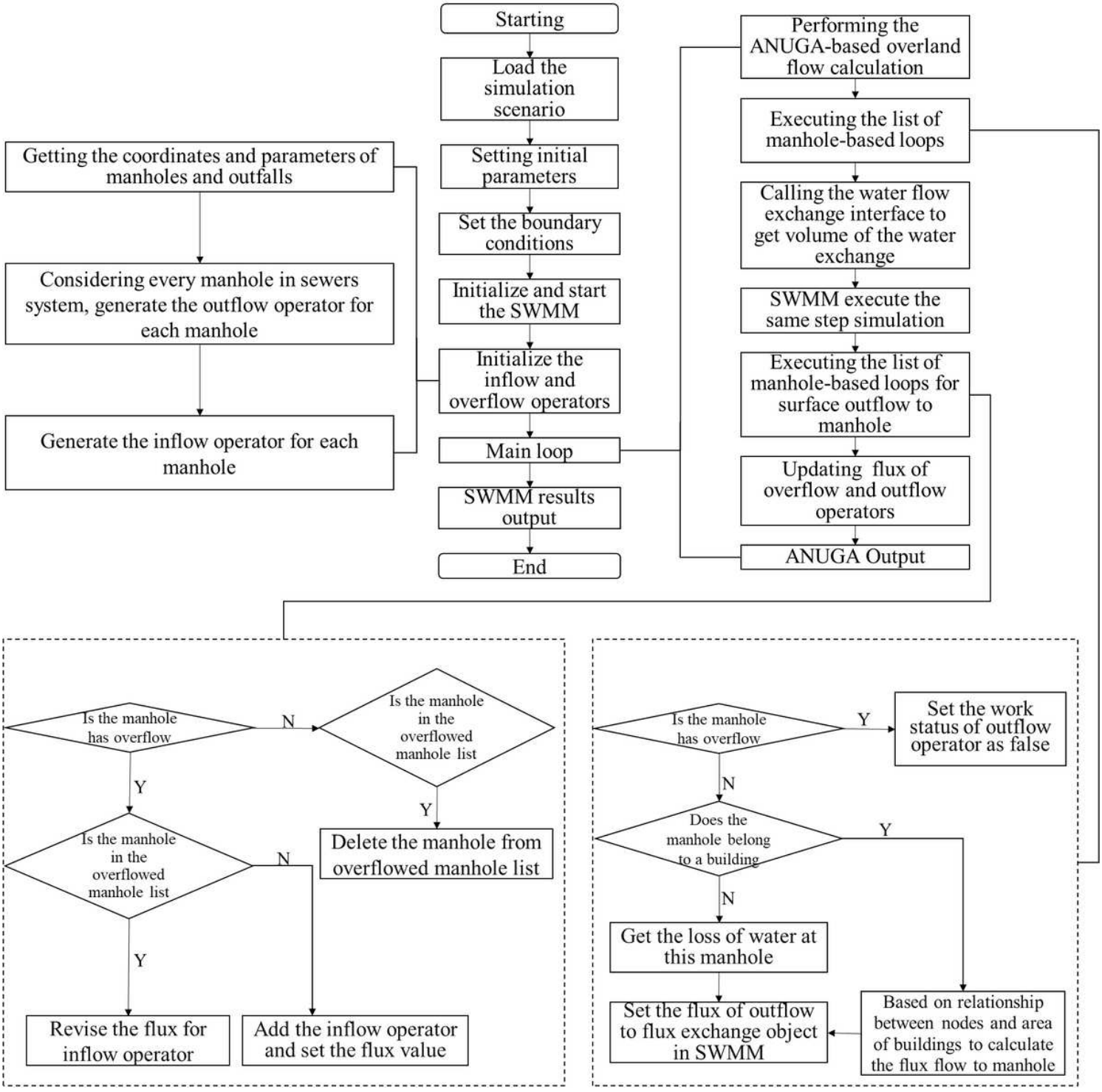

Figure 5

The workflow for the coupled simulation

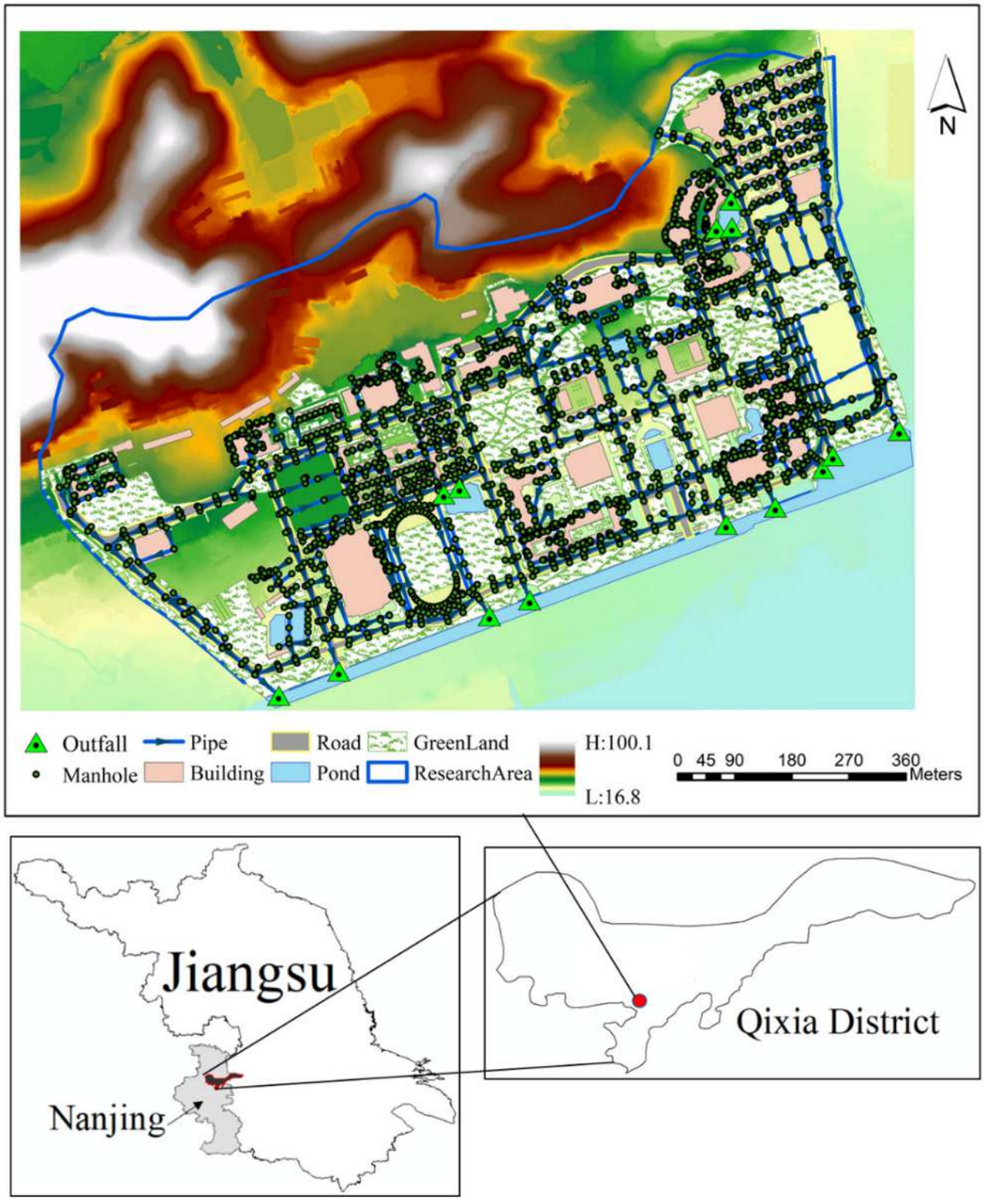

Figure 6

The location of the study area and the basic data Note: The designations employed and the presentation of the material on this map do not imply the expression of any opinion whatsoever on the part of Research Square concerning the legal status of any country, territory, city or area or of its authorities, or concerning the delimitation of its frontiers or boundaries. This map has been provided by the authors.

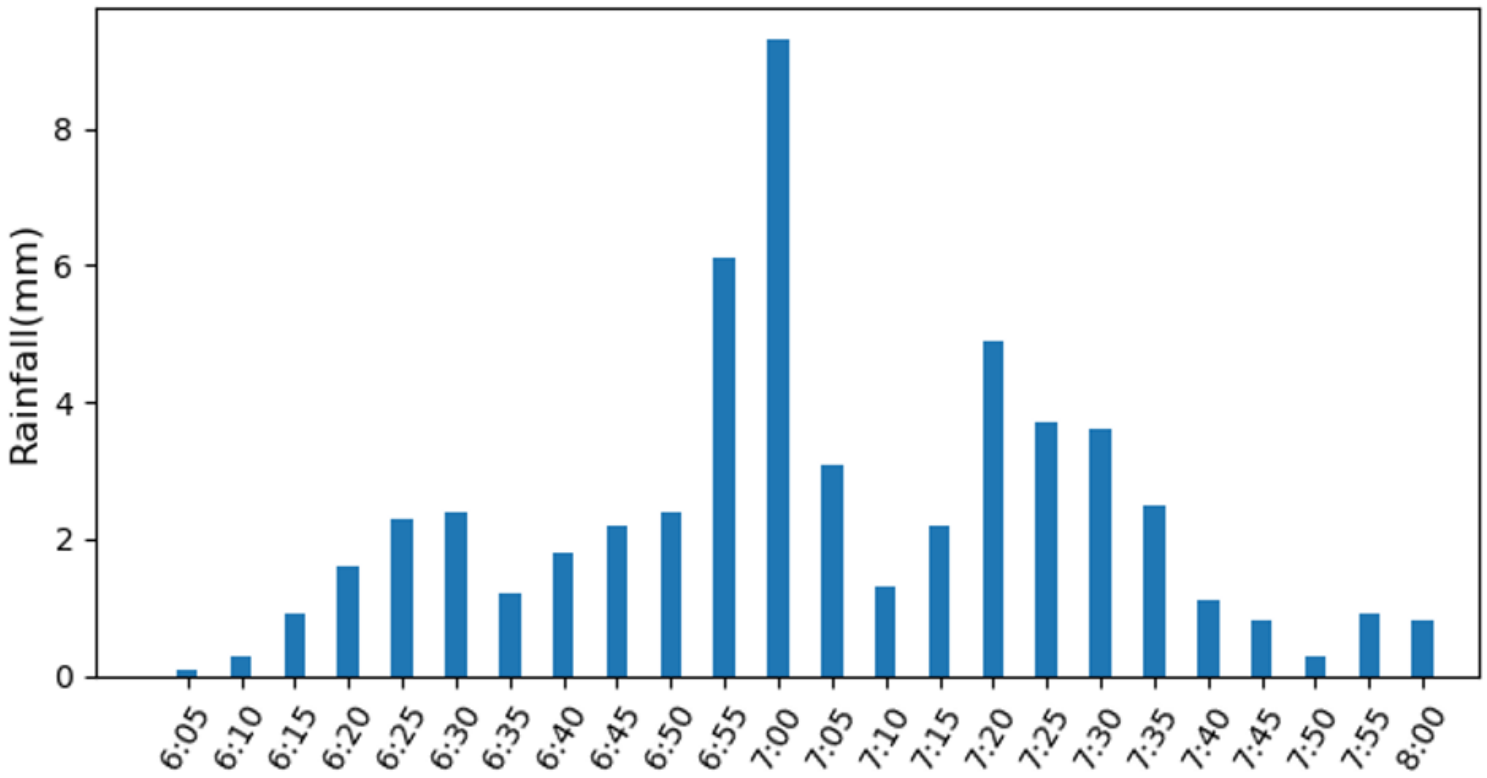

Figure 7

The rainfall time series of the storm event

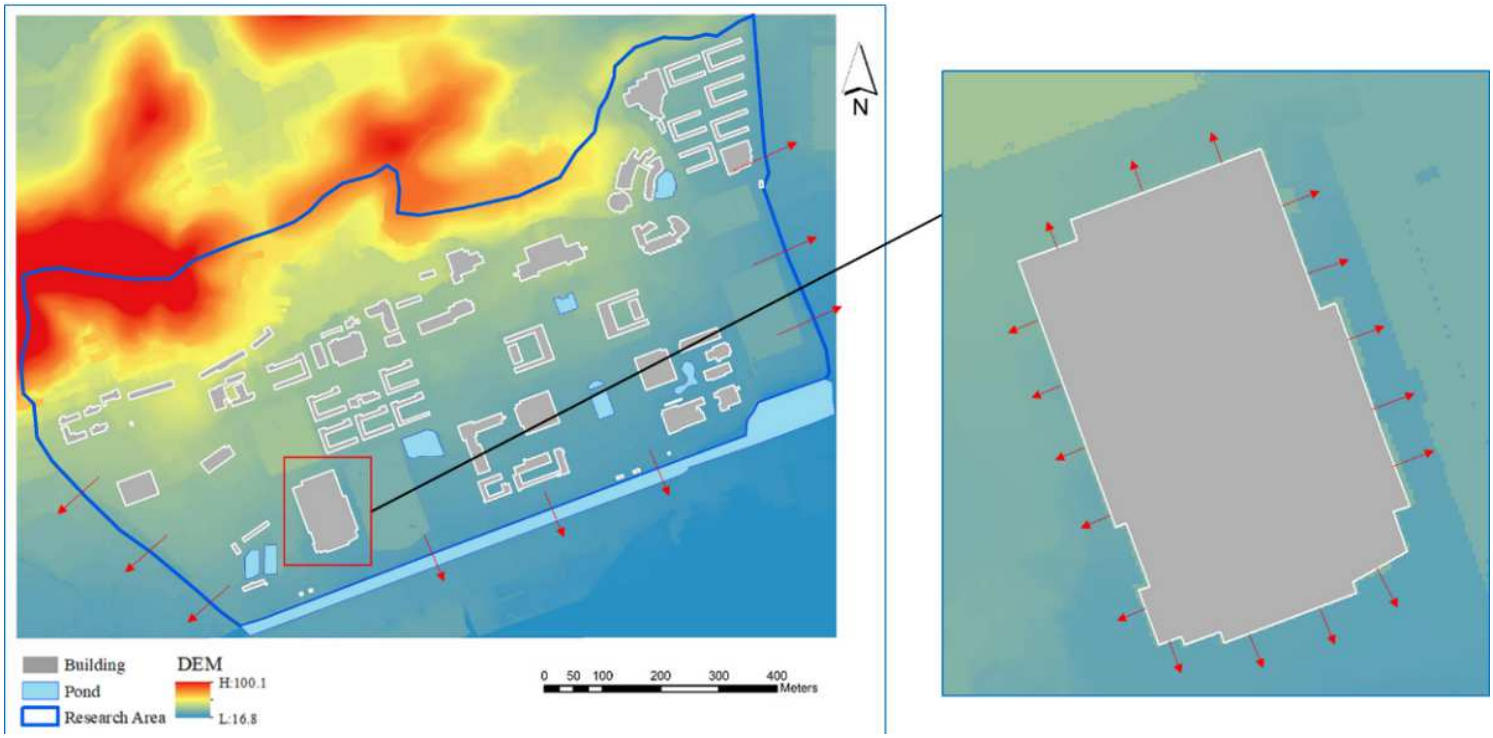

Figure 8

The boundary conditions Note: The designations employed and the presentation of the material on this map do not imply the expression of any opinion whatsoever on the part of Research Square concerning

the legal status of any country, territory, city or area or of its authorities, or concerning the delimitation of its frontiers or boundaries. This map has been provided by the authors.

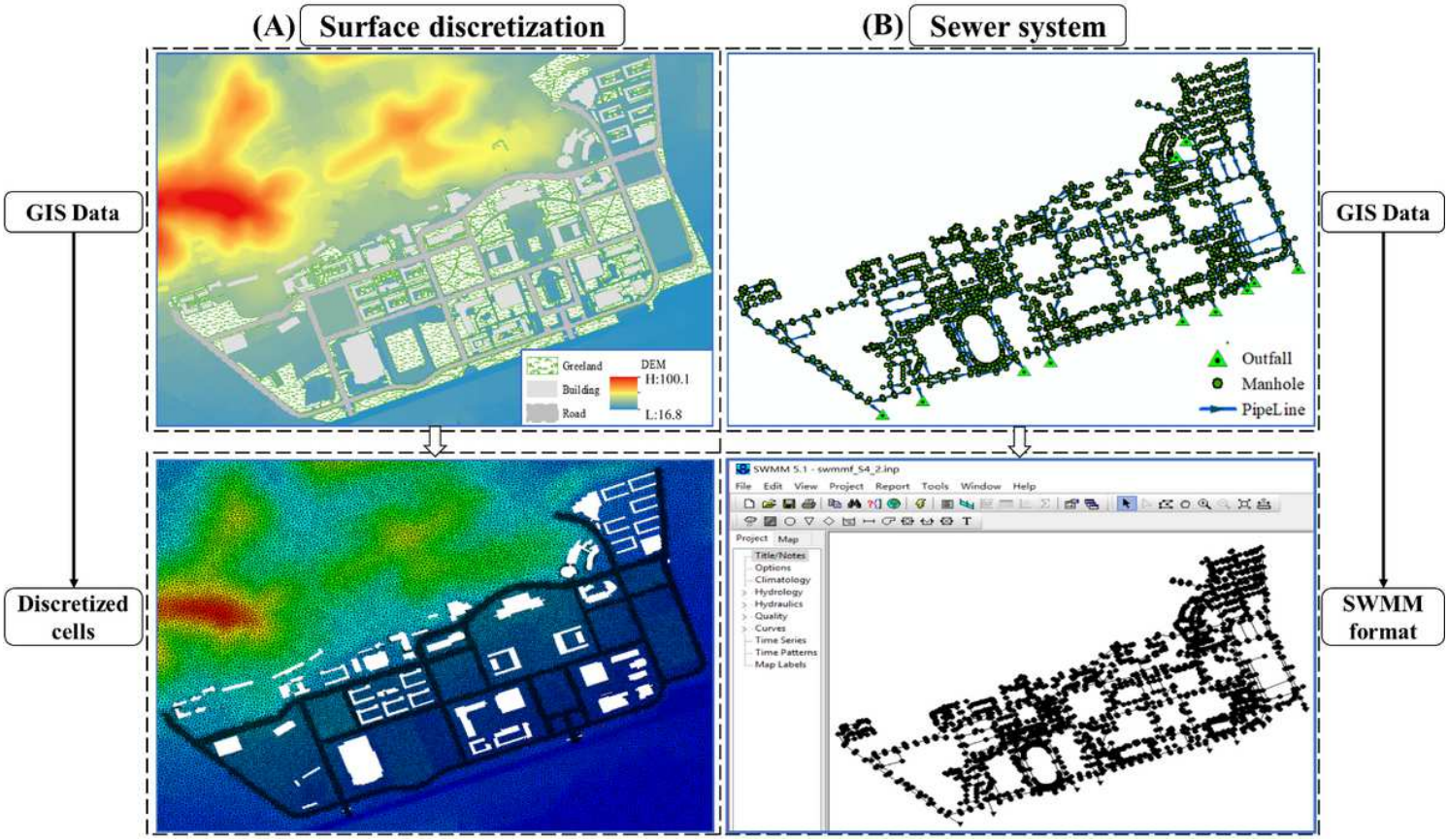

Figure 9

Spatial discretization and data transformation Note: The designations employed and the presentation of the material on this map do not imply the expression of any opinion whatsoever on the part of Research Square concerning the legal status of any country, territory, city or area or of its authorities, or concerning the delimitation of its frontiers or boundaries. This map has been provided by the authors.

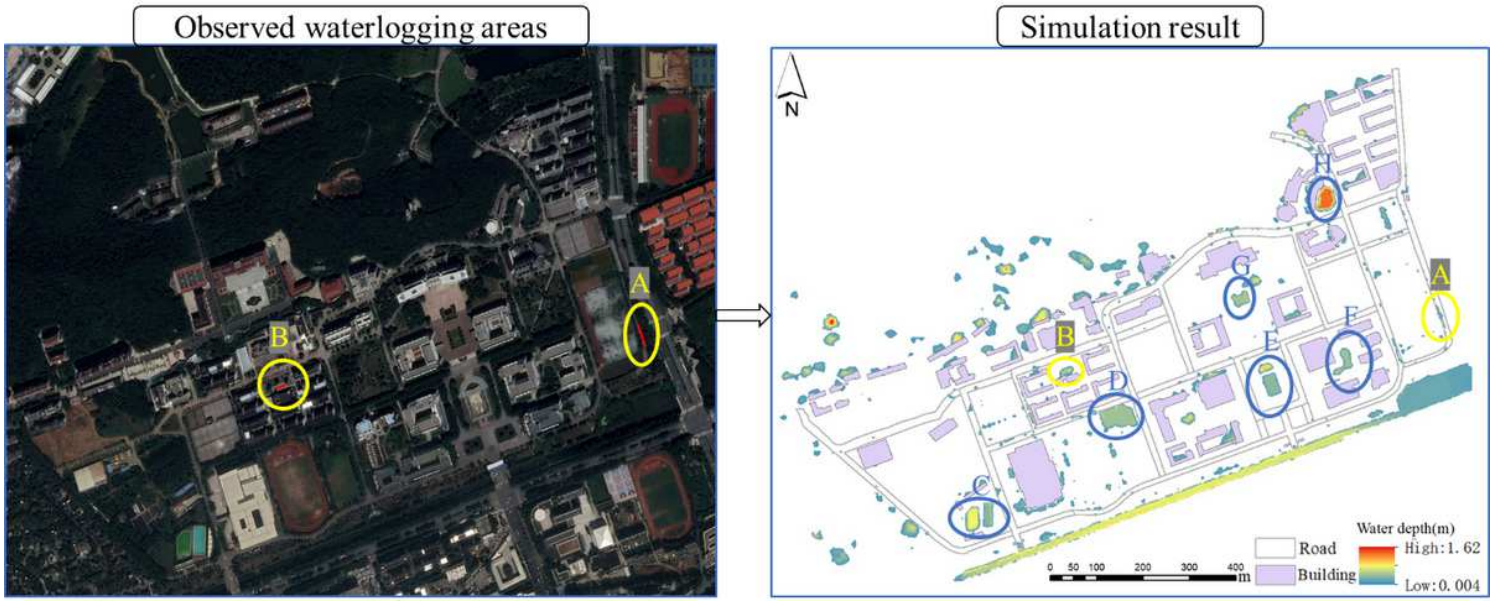

Figure 10

The validation of water-logged locations Note: The designations employed and the presentation of the material on this map do not imply the expression of any opinion whatsoever on the part of Research Square concerning the legal status of any country, territory, city or area or of its authorities, or concerning the delimitation of its frontiers or boundaries. This map has been provided by the authors.

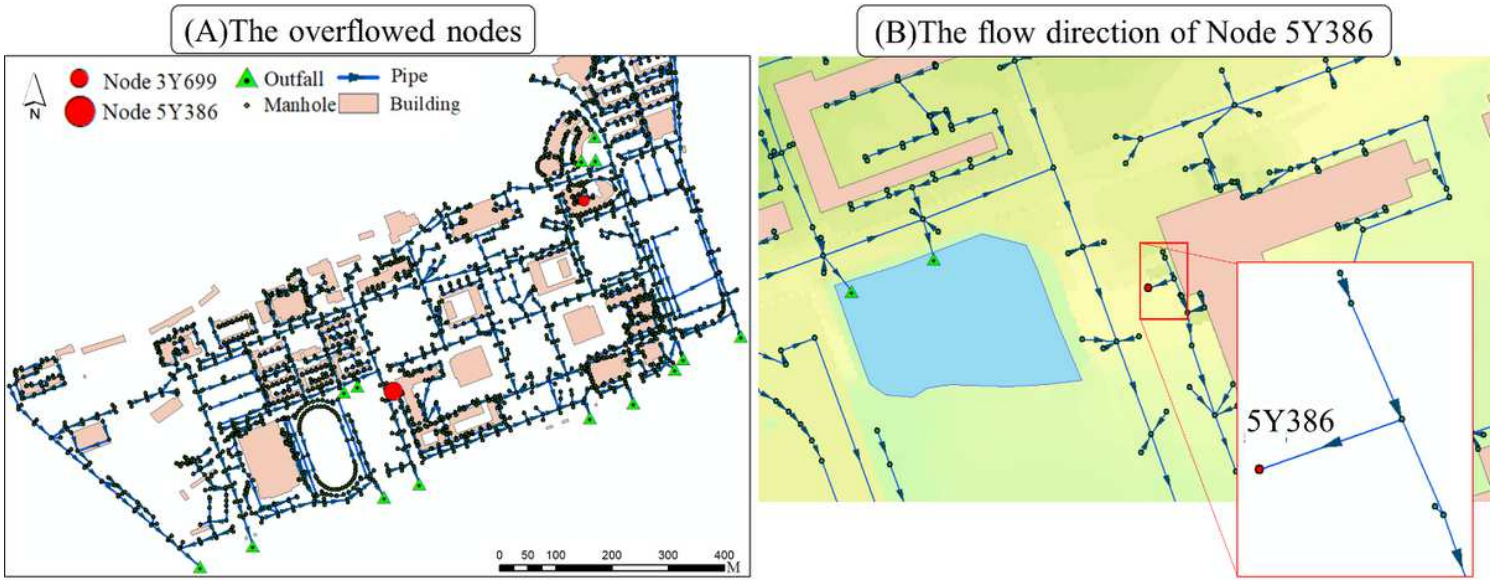

Figure 11

The overflowed nodes and topological relationships Note: The designations employed and the presentation of the material on this map do not imply the expression of any opinion whatsoever on the part of Research Square concerning the legal status of any country, territory, city or area or of its authorities, or concerning the delimitation of its frontiers or boundaries. This map has been provided by the authors.

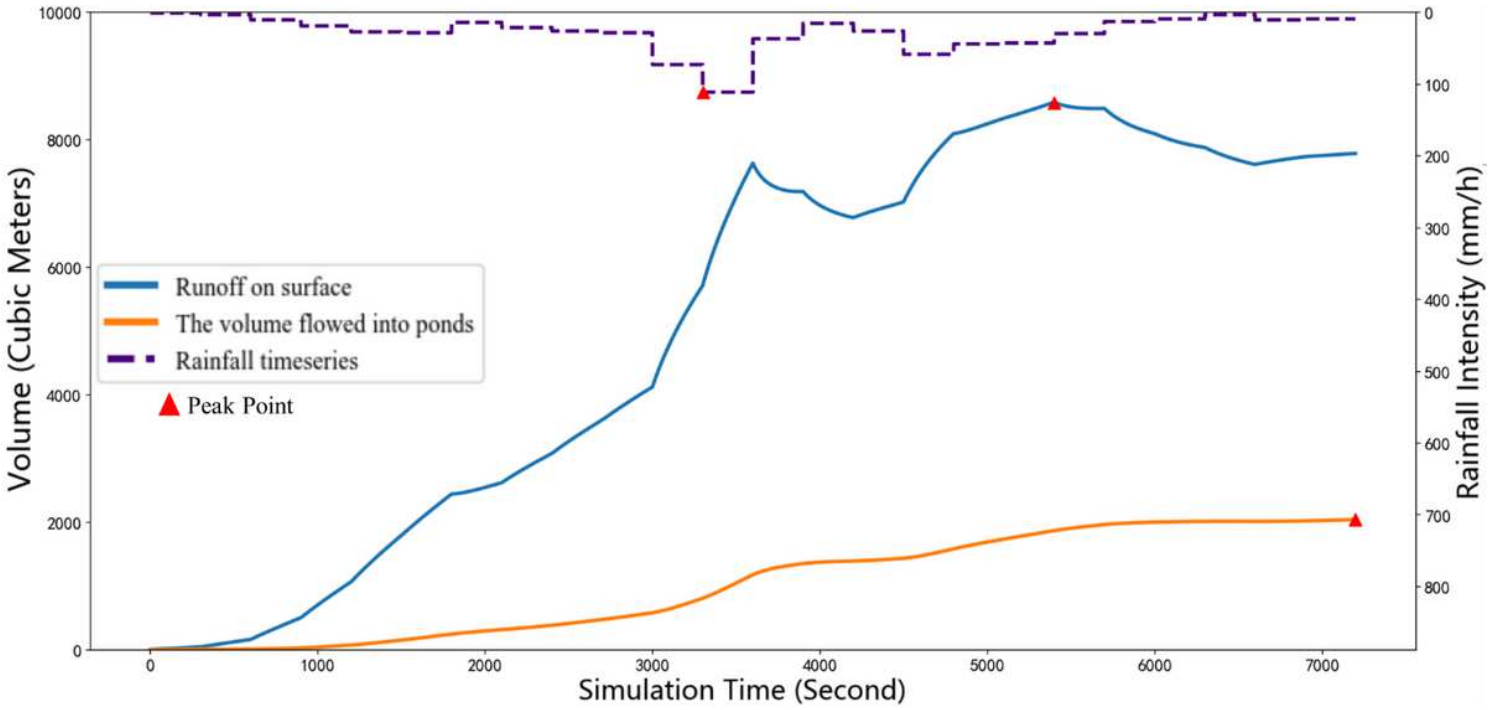

Figure 12

The time series of surface runoff and the volume of pools Note: The designations employed and the presentation of the material on this map do not imply the expression of any opinion whatsoever on the part of Research Square concerning the legal status of any country, territory, city or area or of its authorities, or concerning the delimitation of its frontiers or boundaries. This map has been provided by the authors.

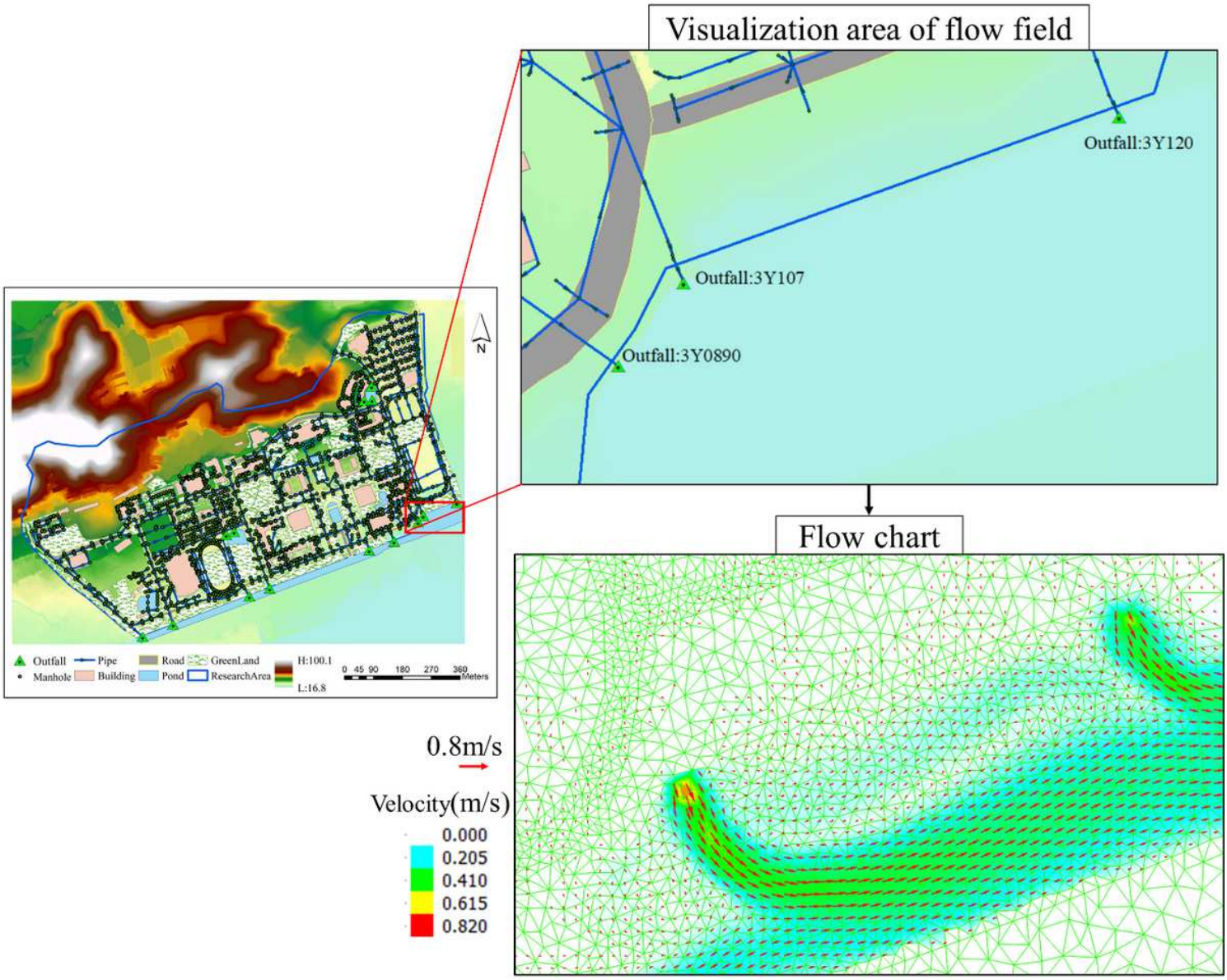

Figure 13

The analysis of the intensity of overland flow Note: The designations employed and the presentation of the material on this map do not imply the expression of any opinion whatsoever on the part of Research Square concerning the legal status of any country, territory, city or area or of its authorities, or concerning the delimitation of its frontiers or boundaries. This map has been provided by the authors.

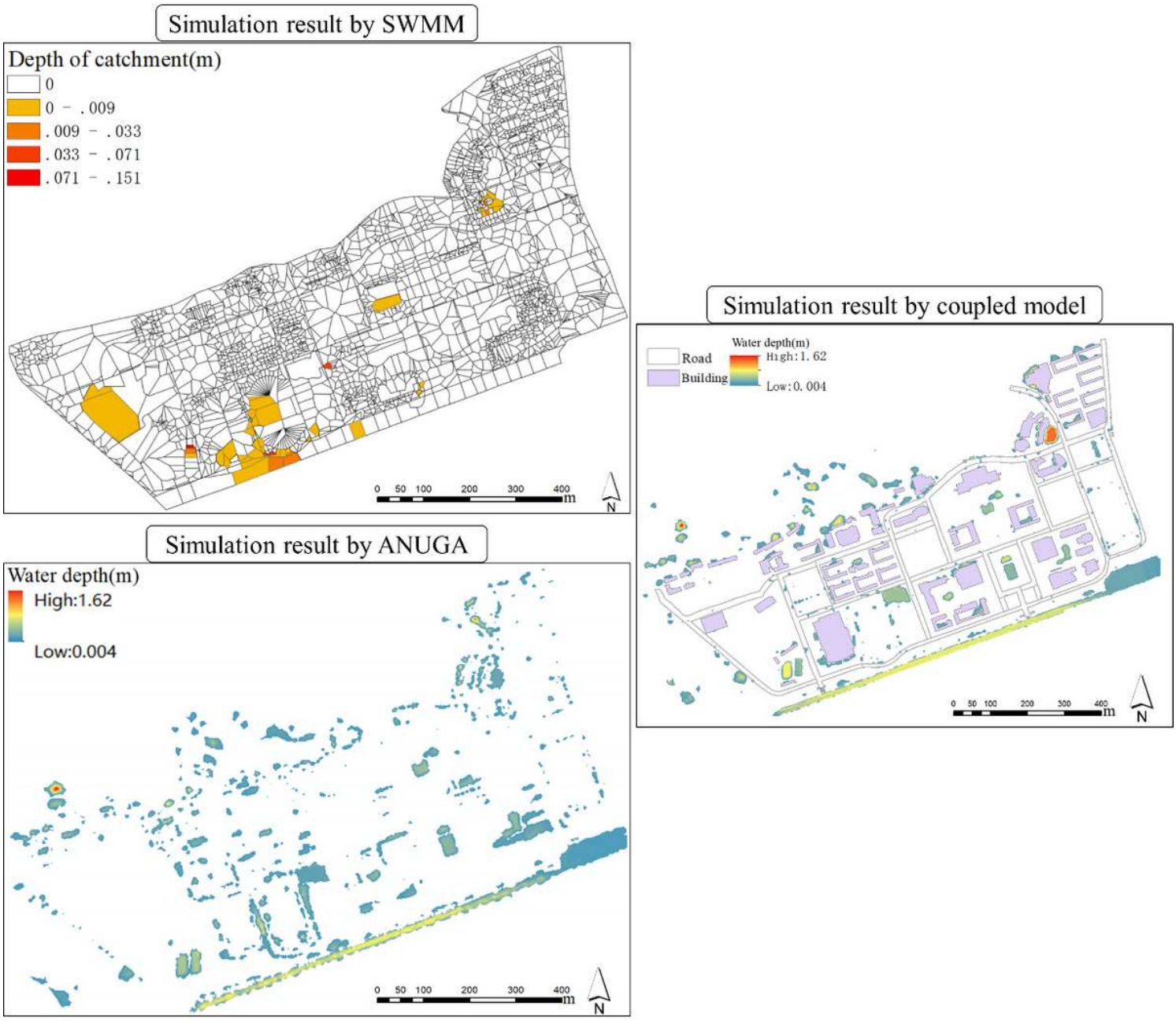

Figure 14

Comparative analysis based on SWMM, ANUGA and the integrated model Note: The designations employed and the presentation of the material on this map do not imply the expression of any opinion whatsoever on the part of Research Square concerning the legal status of any country, territory, city or area or of its authorities, or concerning the delimitation of its frontiers or boundaries. This map has been provided by the authors.